Journal of Hydrology: Regional Studies 67 (2026) 103864

Contents lists available at ScienceDirect

Journal of Hydrology: Regional Studies

journal homepage: www.elsevier.com/locate/ejrh

Future flood and flood-on-drought peaks and volumes in the Northern Apennines through bias-correction and rainfall-runoff transformation of hourly climate forcings

Mattia Neri [a,*], Alfredo Reder [b], Guido Rianna [b], Elena Toth [a]

[a] *Department of Civil, Chemical, Environmental and Materials Engineering, University of Bologna, Bologna, Italy*
[b] *CMCC Foundation - Euro-Mediterranean Center on Climate Change, Caserta, Italy*

A R T I C L E I N F O

Keywords:
Flood events
Flood volumes
Climate projections
Hourly bias-correction
Rainfall-runoff modelling
Compound events
Flood-on-drought events

A B S T R A C T

Study region: Panaro basin, Northern Apennines, Italy.
Study focus: Climate change threatens the resilience of flood protection systems, demanding accurate prediction of flood peaks and volumes and their expected future changes. Particularly, accurate prediction of flood volumes is of paramount importance for operational purposes, such as flood hazard mapping or detention basins. Furthermore, abrupt shifts from extended dry periods to floods pose significant challenges to regional early warning systems. Predicting future flood events is particularly challenging over small and mid-sized catchments, characterised by response times of a few hours, where both long time-series of past hydrometeorological observations and future projections at fine time scale are needed. The work proposes a methodology for the reliable simulation of past and future flood occurrence and magnitude, in terms of flood peaks and volumes. It relies on continuous streamflow simulation through i) hourly bias-correction of regional climate projections, ii) rainfall-runoff modelling and iii) a peak-over-threshold approach for flood characterisation. Moreover, a novel combination of metrics for analysing the evolution of compound flood-on-drought events is tested.
New hydrological insights: The hourly bias-correction approach effectively adjusts the ensemble of regional climate models, allowing accurate reproduction of the flood regime. Simulations project a decrease in the frequency of flood events, but higher flood peaks and volumes are expected. In contrast, future compound drought and flood events are projected to become more frequent.

1. Introduction

Dry and wet climate extremes are occurring more frequently and with increasing severity (Barendrecht et al., 2024; Rodell and Li, 2023) and are expected to become even more frequent and intense with ongoing climate change (IPCC, 2023).

The evaluation of the resilience of flood protection measures requires an assessment of the impact of climate change scenarios on future flood regimes (Hall et al., 2014; Tarasova et al., 2023), focusing on different flood features and not only on the expected peaks. In particular, the prediction of flood volumes and their expected changes in future decades is essential for a number of operational purposes, such as, for example, the design of detention basins or flood hazard mapping, and it requires specific analyses. In fact, the

* Corresponding author.
E-mail address: mattia.neri5@unibo.it (M. Neri).

https://doi.org/10.1016/j.ejrh.2026.103864
Received 9 April 2026; Received in revised form 10 August 2026; Accepted 11 August 2026
Available online 26 August 2026

reliability of a model in predicting other flood characteristics, as flood peaks, does not necessarily translate into accurate flood volume prediction (e.g. Peredo et al., 2022). For this reason, a number of recent studies has focused specifically on projecting trends in flood volumes under climate change (e.g. Dankers and Feyen, 2008; He et al., 2022; Ho et al., 2022; Ionno et al., 2024).

At the same time, along with the characterisation of flood volumes regimes, the study of the occurrence of abrupt hydrological extremes changes, and in particular the shift from extended dry periods to flood events results of particular interest for the stakeholders dealing with the operational management of environmental hazards. Recently, the time interval between consecutive drought and flood events has been shown to be decreasing in certain areas across the globe, implying that there is less time to recover from the impacts of a dry event before a flood occurs (He and Sheffield, 2020; Rashid and Wahl, 2022; Rezvani et al., 2023). In fact, when floods occur during or soon after drought periods, early warning systems can become inaccurate (e.g. Fowler et al., 2020; Matanó et al., 2024) and water management practices may fall short in reducing the risk of both extremes (e.g. Ward et al., 2020). Therefore, when assessing the impact of climate change on flood regimes, the expected changes in the interaction with the occurrence of drought events should be also taken into account. In addition, in some regions around the world, like the Mediterranean, the need to assess expected shifts in flood regimes and their nexus with periods of water scarcity is increasingly urgent, given that climate models often lack consensus on projected changes to meteorological forcings and their seasonality (e.g. Todaro et al., 2022).

Assessing the evolution of flood events over past and future decades over the small and mid-sized catchments of Northern Apennines, characterised by response times of a few hours is extremely challenging (e.g. Evin et al., 2024; Ficchì et al., 2016) due to the frequent lack of long series of past observations at fine temporal resolution (sub-daily). Historical hydrometeorological time series at fine temporal scale are necessary and should be sufficiently long not only to better understand the long-term regimes of the meteorological and hydrologic variables characterising floods, but also to be used as reference to validate and adjust climate model projections, needed to simulate future meteorological forcings. In fact, although the developments in dynamical downscaling have contributed to a more robust model assessment of the future climate (Christensen et al., 2019), 'bias-correction' approaches are still required in many cases. So far, such techniques have been applied principally to daily climate simulations with satisfactory results in climate change impact studies, when using climate simulations as forcings to daily rainfall-runoff modelling chains (see e.g., among many others, Castaneda-Gonzalez et al., 2022; D'Oria et al., 2019; Kay, 2022; Majone et al., 2016; Peres et al., 2019; Perra et al., 2018; Peßenteiner et al., 2021; Senatore et al., 2022). On the other hand, in recent years, an increasing number of GCM-RCM simulations at sub-daily (3 or 6 h) or even hourly scales have become much more widely available (e.g. Raffa et al., 2023 for Italy), and it is therefore interesting to analyse the performance of bias-correction procedures applied at such fine-scale. Such analyses are, so far, very limited in the literature and mainly focussed on bias-correction approaches applied not to the entire time series but only to the design extreme rainfall values (e.g. Li et al., 2017; Requena et al., 2021). In fact, when considering dynamics with a modest dependence on the hydrological conditions preceding the event, such as pluvial floods in urban areas, bias correction can be applied directly to the intensity-duration-frequency (IDF) curves or on predefined thresholds (e.g. Padulano et al., 2019; Srivastava et al., 2021). For evaluating, on the other hand, the future regime of riverine floods, it is crucial to take into account also the antecedent conditions through the evolution of the hydrological state variables that represent the memory of the basin functioning: to do so, there is the need for continuous climate input time-series, representing both storm and inter-storm periods, to be used as forcing to a continuously-simulating rainfall-runoff model.

To date, applied studies on bias correction approaches on whole series of atmospheric variables at sub-daily scales and with the purpose of simulating rainfall-runoff propagation processes are still quite limited in the literature (notable exceptions are Brunner et al., 2021; Faghih et al., 2021; Poncet et al., 2024; Reszler et al., 2018; Ye et al., 2023), both because the wide availability of climate simulations at this fine scale is recent and because of the frequent lack of long series of sub-daily measurements, which are needed for an effective assessment of historical inter-annual variability over the control periods.

This study aims to contribute to the characterization of expected changes in flood regime and their nexus with periods of hydrological droughts in an Italian region located in the Northern Apennines, which recently experienced unprecedented flood events in 2023 and 2024 (Brath et al., 2023; Di Paola et al., 2026; Foraci et al., 2023), while one of the most severe droughts of the last century was still in progress (Biella et al., 2025; Montanari et al., 2023). The study is applied to a representative mid-sized headwater catchment, the Panaro river (a tributary of the Po river), which is of particular interest as it is located upstream of a flood retention system, making the accurate estimation of flood volumes essential for its effective operational management.

The first phase of the work involves the assessment of past and future patterns of flood occurrence and magnitude, focusing on both flood peaks and volumes. To this aim, the Scaled Distribution Mapping (SDM) approach, proposed and applied on daily time-series by Switanek et al. (2017), is especially adapted to the whole series of hourly meteorological forcings of an ensemble of regional climate projections. Afterwards, two continuously-simulating and conceptual rainfall-runoff models are parameterised and then run to reproduce the streamflow time-series in the study river. The effectiveness of the bias-correction approach for the simulation of the streamflow over the control period is evaluated focusing on the reproduction of historical flood characteristics (occurrence, flood peaks and volumes) which are used as reference to analyse their expected changes over the future decades.

Secondly, the work aims to capture, based on the proposed modelling chain, the future evolution of hydrological droughts in the study area and their nexus with the occurrence and magnitude of floods. Literature about abrupt shift from dry to extreme wet periods mainly focuses on transitions in meteorological states (e.g. Ansari and Grossi, 2022; Liu et al., 2018; Shi et al., 2021; Yang et al., 2013) while, in contrast, little is known about consecutive or compound hydrological drought and flood events (Brunner, 2023): the few existent studies focus on the understanding of the hydrological and/or socio-economic processes underlying drought-to-flood interactions and dynamics (e.g. Barendrecht et al., 2024; Parry et al., 2016), rather than on their future evolution. Notable exception is the work of Matanó et al. (2024) which explored historical occurrences of compound or consecutive drought and flood events and the effects of droughts on flood severity and timing at a global scale. Here, we propose and test a framework to detect the occurrences and features of compound flood-on-drought events, that is floods occurring during droughts for both the historical and future periods, analysing their expected changes.

The manuscript is organised as follows: while 2 briefly describes the study region, 3 is dedicated to the collection, processing and validation of historical climatic data. Rather than separating methods and results, Sections 4 through 6 integrate the methodology and corresponding results for each phase of the analysis. Specifically, 4 describes the bias-correction approach applied to the selected hourly regional climate projections and its results; 5 presents the hydrological modelling strategy and reports the obtained simulations of past and future flood peaks and volumes; in 6, the future evolution of flood-on-drought events is analysed. Finally, in 7 the results are discussed and 8 draws the conclusions of the study.

2. Study region

The Panaro river rises in the northern Apennines mountains, and it is the last tributary of the Po river. The downstream part of the river has always been affected by flooding events that have caused devastating damages in the past decades.

A temperate climate characterises the region, but annual precipitation varies remarkably, from around 500–700 mm in the Po valley to more than 2000 mm in the highest mountain areas. Average daily temperatures range between −2 °C and 4 °C in winter and between 15 °C and 24 °C in summer, respectively, for the mountain and valley areas.

The present study focuses on the mountain and hill portion of the Panaro watershed, where most of the runoff is generated. In particular, the headwater catchment closed at the river section of Spilamberto, covering an area of 747 km^2, is considered for the analyses. The left panel of Fig. 1 shows the catchment border (black line) within the hydrological network of the Po river in northern Italy. Such catchment is of particular interest because its outlet corresponds to the last stream gauge (i.e. hydrometric station) upstream to the Sant'Anna flood retention system, and the river discharge observation in this section is used by the Po River Authority ("Agenzia Interregionale per il fiume Po", AIPO) to estimate the inflow to such retention basin.

Based on the hourly discharge records available from 2006 to 2015 (provided by the regional meteo-hydrological service SIMC-ARPAE), the average annual discharge at Spilamberto is around 16 m^3/s. The flow regime is nearly ephemeral, with summer values close to zero and high flows (annual hourly maxima vary between 150 and almost 900 m^3/s in the observation period) occurring generally in the fall and early winter months. On average, more than ten events per year exceed 64 m^3/s (corresponding to the 95th quantile of hourly discharges).

3. Historical climatic data

Past meteorological observations are essential to estimate precipitation and temperature spatial fields needed both to force the hydrological model used to simulate the river discharge at the basin outlet and as the reference to bias-correct and validate the regional climate models.

Considering the purpose of the proposed approach, measures at hourly time step are indeed needed. Retrieving hourly meteorological time series is always challenging: on the one hand, the availability of ground measures is generally limited in space and time; on the other, alternative products (i.e. gridded datasets) are often not accurate at such fine temporal resolution, and their reliability has to be preliminarily verified.

The meteorological sensors are owned and managed by the regional meteo-hydrological service (SIMC-ARPAE). The network of rain gauges is quite dense (right panel of Fig. 1): the number of measures across the network is good enough to guarantee the

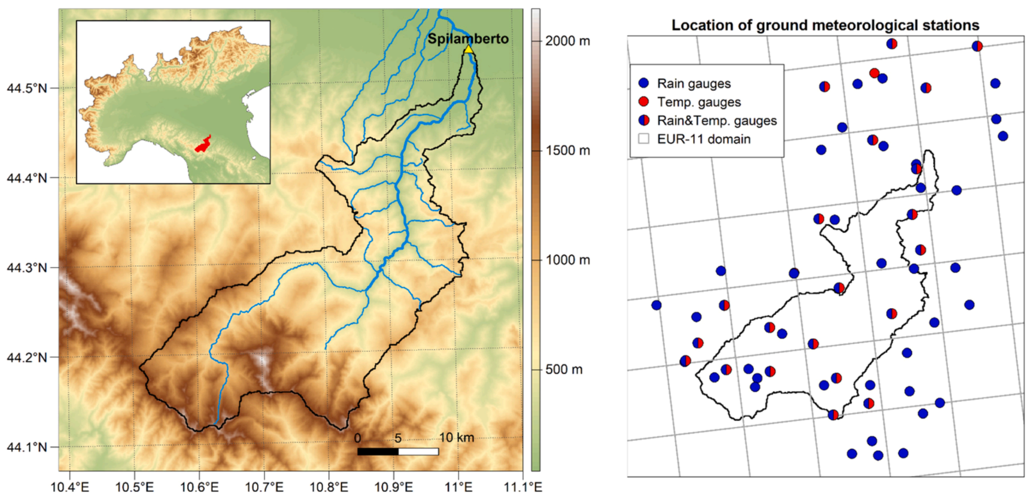

Fig. 1. Study region. Left: the Panaro basin (black contour) closed at the Spilamberto river section gauge. Right: location of available rain and temperature gauges across the study area (EUR−11 cordex grid domain is also showed).

computation of reliable hourly precipitation fields from 1995 to present. Temperature gauges instead are less and allow to properly estimates hourly temperature fields from 2003 to present. Detailed description of ground measures availability over the historical period is reported in the Supplement (Section S1).

Spatial interpolation of ground measures is carried out for obtaining the spatial averages of precipitation and temperature fields over the study domain. In a preliminary analysis conducted on the study area (not reported here), methods among the most consolidated in the literature, were tested in cross-validation. For precipitation, a simple inverse distance weighted method with a cubic power distance is chosen, which was shown to provide satisfactory results when tested in cross-validation. The method leading to the most accurate estimate of air temperature and thus selected for the spatial interpolation, was a linear regression with elevation (see, e.g. Stahl et al., 2006). Spatial interpolation of ground measures is performed over a high-resolution 80 × 80 m grid, allowing for subsequent spatial averaging over either the basin domain or a coarser grid (e.g. the RCM domain).

The period of records for which the ground measures are available (1995–2019 for rainfall and 2003–2019 for temperature) is certainly long enough to calibrate and run a rainfall-runoff model. However, it covers only part (16 or 8 years, respectively) out of the 30 years of the "historical experiment" (i.e. control period 1981–2010) generally used in the bias-correction approaches for the RCM-GCM modelling chains, in line with the World Meteorological Organization guidelines (WMO, 2017).

In order to explore the possibility of obtaining a longer observation period (closer to the typical length of the "control period"), gridded meteorological products available over Europe have been analysed. In particular, the ERA5-Land dataset (Muñoz-Sabater et al., 2021) at hourly resolution is here considered as an alternative option. The details about characteristics, processing and validation of ERA5-Land are reported in the Supplement (Section S1). Here, for the sake of brevity, we report a summary of the analysis.

Precipitation and temperature fields included in such datasets are compared to those retrieved from the available ground hourly measures across the basin through the spatialization procedure described above. In particular, hourly basin mean areal precipitation (MAP) in years 1995–2019 and mean areal temperature (MAT) in years 2003–2019 (periods with the highest density of ground stations) are computed for the ERA5-Land product and compared with those obtained from the spatialization of ground measures.

Unfortunately, a poor match is observed between gauged-derived and ERA5-Land hourly MAP estimates (Pearson correlation around 0.55). Even if the match of daily values slightly improves with respect to the hourly ones, Pearson correlation remain below 0.80, highlighting a limitation of the capability of ERA5-Land product in the reproduction at the daily scale over the study region (see additional details in Section S1). This confirms the high spatial variability of the accuracy of ERA5 products which should be always verified, as demonstrated by a number of previous studies which reported either acceptable (Clerc-Schwarzenbach et al., 2024; Klingler et al., 2021; Tarek et al., 2020) or poor (e.g. Cammalleri et al., 2024; Lavers et al., 2022; Longo-Minnolo et al., 2022; Sarigil et al., 2024) accuracy of its precipitation estimates.

As far as temperature is concerned, the correspondence between hourly simulated and observed values is much better than for precipitation, even if ERA5-Land tends to underestimate temperatures. Differently from the rainfall data, temperature data have much less intraday variability than precipitation and the use of daily data (maximum and minimum along the day) to estimate the diurnal cycle of hourly data is a widely applied and generally reliable practice. For this reason, the use of daily maximum and minimum temperature from the E-OBS dataset (Cornes et al., 2018), based on ground observation, is also taken into account. Hourly temperature estimates are derived from E-OBS minimum and maximum daily values with the interpolation method proposed by Linvill (1990), averaged over the basin domain, and compared to gauged-derived hourly temperatures, revealing a very good correspondence, with a very weak overestimation of hourly values (see Section S1 in the Supplement for details).

Finally, for the bias-correction of the regional climate projections and the rainfall-runoff simulation, given the lack of reliability of the ERA5-Land precipitation estimates over the study region, hourly rainfall fields interpolated from the ground gauges are taken as references, even if available only from 1995 onwards. Regarding temperatures, we opted to use hourly E-OBS-derived estimates, which cover the entire historical control period and exhibit a significantly smaller bias against observations compared to ERA5-Land.

4. Climate scenarios and hourly bias-correction over the control period

The capabilities of the current generation of Global Climate Models (GCMs), although greatly improved through advances in computing power and representation of physical dynamics (Wilby, 2017), are widely acknowledged to not allow for proper characterisation of weather dynamics at regional and local scales. A step towards refining climate projections is to localise GCM results using higher resolution Regional Climate Models (RCMs) nested over the area of interest on the GCM from which they retrieve boundary conditions. RCMs make it possible to better characterise geomorphological features (e.g. orography, land-sea interaction, land-use effects) and to explicitly evaluate different weather dynamics that are parameterised as sub-grid processes in GCMs. As already mentioned, the main limitation of RCMs, whose resolution varies between 10 and 50 km, is generally attributed to the use of parameterizations for simulating convective processes. Such parameterizations may lead to inaccurate modelling of sub-daily precipitation (Kendon et al., 2017), which is essential for simulating flood phenomena in mid-sized, mountainous basins (see, e.g., Berg et al., 2019; Kendon et al., 2021). Convection-permitting regional climate models (CP-RCMs) can more accurately represent sub-daily statistics and extremes (e.g., Adinolfi et al., 2023; Dallan et al., 2023; Fosser et al., 2015; Reder et al., 2022), providing greater confidence in their climate projections compared to traditional RCMs (e.g. Fosser et al., 2024; Pichelli et al., 2021). However, due to the limited availability of CP-RCMs projections, both in terms of spatial and temporal coverage, typically spanning only 10–20 years (with few exceptions, see e.g. Kendon et al., 2019; Raffa et al., 2023), the simulations of state-of-the-art regional climate models are still the most-widely used for real-world climate services (such as the EURO-CORDEX 0.11 ensemble that is used in the present work).

This Section first introduces the RCMs selected for the study; then, it outlines the method implemented to reduce biases in the climate simulation chains; finally, it presents the differences between raw and bias-adjusted climate data using observations as reference for recent climate, also giving indications on future climate signals returned by RCMs.

4.1. Selection of GCM-RCM modelling chains

This study takes advantage of the GCM-RCM coupled simulations available within the Coupled Model Intercomparison Project 5, specifically utilizing the EURO-CORDEX ensemble. It is worth noting that the EURO-CORDEX dataset represents an “ensemble of opportunity” where not all the error sources can be adequately accounted for and quantified; therefore, it could represent a sort of lower boundary of the uncertainties affecting the evaluation of future evolution in weather forcing.

Within this perspective, the idea behind the selection of the climate simulation chains (listed in Table 1) is to share the same Representative Concentration Pathway (RCP) and the same RCM with the same parameterisation, in order to clearly appreciate the effect of the differences among the driving GCMs. Consequently, a set of six hourly climate simulation chains (GCM-RCM) was selected, all corresponding to the highest-emission scenario (RCP8.5). For the regional downscaling, the SMHI-RCA4 model (Samuelsson et al., 2011; Strandberg et al., 2014) was chosen because it provided, to the best of the authors’ knowledge, the largest homogeneous set of EURO-CORDEX hourly chains available for the required variables and periods.

This specific setup carries some limitations. RCM structural uncertainty is not explicitly sampled, since all chains use the RCA4 model, and alternative emission scenarios are not explored. The projections should therefore be read as conditional on this RCA4-based high-emission ensemble, and not as a full probabilistic assessment of future changes. Nevertheless, the selected subsample provides a robust representation of GCM-driven variability, as it includes models characterised by widely different Equilibrium Climate Sensitivity (ECS), that is, the equilibrium change in annual global mean surface temperature that follows a doubling of the atmospheric concentration of carbon dioxide with respect to pre-industrial levels.

We acknowledge that CMIP6-based regional information is increasingly available through statistical downscaling products, including high-resolution datasets also over Italy (Fedele et al., 2025). First CMIP6-based dynamical downscaling experiments over Italy are also emerging (Vichot-Llano et al., 2026). However, these products remain limited for the purposes of the present application, either because of their daily temporal resolution or because they do not yet provide a long multi-model ensemble of sub-daily simulations. Convection-permitting models provide a further benchmark for sub-daily precipitation extremes, as they better represent intense and localised events than conventional RCMs (Fosser et al., 2024; Raffa et al., 2023), but their use here is also limited by shorter simulation periods and by the lack of long multi-model ensembles suitable for robust uncertainty assessment.

4.2. Bias-correction procedure

Bias adjustment is often necessary for estimating climate, as raw outputs are usually biased against average statistics of observations over a shared control period. Part of these biases derive from the parent GCM; others are related to the modelling formulation and physical parameterizations of the adopted RCM.

One of the most widespread strategies to minimise these biases relies on the use of statistical bias correction methods. In short, bias correction includes "any method that establishes a statistical transfer function between the model and the observed data and applies this transfer function to the post-processing model data" (Maraun and Widmann, 2018). In the literature, different methods have been developed (Casanueva et al., 2020; Maraun, 2016; Maraun et al., 2010; Spuler et al., 2024; Switanek et al., 2017; Teutschbein and Seibert, 2012) and applied to post-processing climate projections. A widely used method is quantile-quantile mapping (QM, Piani et al., 2010; Themeßl et al., 2011), that adjusts the cumulative density function (CDF) of the modelled variable so that it becomes identical to the CDF of the observations.

Recent studies reveal that this type of bias correction may however artificially alter in a significant way the climate change “signal” that is predicted from the raw climate models for the future decades due to the stationarity assumption for which the same error-correction function calculated for the calibration period is applied to any future period of interest (Maurer and Pierce, 2014; Switanek et al., 2017; Themeßl et al., 2012).

Recently, modifications of the standard QM method have been developed to force the preservation of the climate change signal projected by the raw model, like the Detrended Quantile Mapping (DQM, Hempel et al., 2013) or the Quantile Delta Mapping (QDM, Cannon et al., 2015). In the present study, raw RCM outputs are corrected using the Scaled Distribution Mapping (SDM) method (Switanek et al., 2017) which is aimed at preserving the projected changes in climate signal identified by the raw RCMs between control and future periods across the entire distribution. This feature is particularly relevant here, since the corrected hourly forcings are used to assess future changes in flood occurrence, peaks and volumes. Operatively, the SDM fits a specific parametric distribution to

Table 1
List of climate simulation chains used in this work. ECS values are retrieved from Meehl et al. (2020) and Wyser et al. (2020).

Institute	RCM	Driving GCM	ECS (°C)	CORDEX full name	Chain Acronym
SMHI	RCA4	MPI-M-MPI-ESM-LR	3.6	MPI-M-MPI-ESM-LR_r1i1p1_SMHI-RCA4	CM1
		MOHC-HadGEM2-ES	4.6	MOHC-HadGEM2-ES_r1i1p1_SMHI-RCA4	CM2
		CNRM-CERFACS-CNRM-CM5	3.3	CNRM-CERFACS-CNRM-CM5_r1i1p1_SMHI-RCA4	CM3
		ICHEC-EC-EARTH	3.3	ICHEC-EC-EARTH_r1i1p1_SMHI-RCA4	CM4
		IPSL-IPSL-CM5A-MR	3.5	IPSL-IPSL-CM5A-MR_r1i1p1_SMHI-RCA4	CM5
		NCC-NorESM1-M	2.8	NCC-NorESM1-M_r1i1p1_SMHI-RCA4	CM6

the data and, to correct the future modelled values, scales the observed distribution on the basis of the distance between the two CDFs obtained from the raw model simulations over the control period and the future period. For precipitation series, it also takes into account the projected change in the frequency of rainy days. In the hourly implementation adopted here, this corresponds to correcting the mismatch between observed and modelled wet-hour frequency in the calibration period, while preserving the projected control-to-future change in wet-hour frequency. No assumption of stationarity is made during bias correction since the scaling between model simulations and observations changes depends on the bias correction period.

There are a few important differences between the implementation of the SDM for precipitation and temperature. First, SDM scales the distribution of precipitation by a multiplicative (or relative) amount, and temperature is scaled by an absolute (delta) amount. Second, only values of positive precipitation exceeding a specified threshold (e.g. 1 mm for daily precipitation) are used to build the distributions of the rainfall depths (since they refer only to the rainy days), while all temperature values are used. Third, the temperature data belonging to any considered 3-decades period (past or future) is first detrended, then bias corrected, and finally, the trends are added back in. As a result, the variance is not inflated by temporal trends that are expected in each decade.

The SDM was originally developed to adjust daily time series (precipitation depth and temperatures). In this study, it is instead adopted to correct the modelled hourly precipitation and the daily maximum and minimum temperatures for all the grid cells falling in the investigated domain. It is therefore used to correct precipitation time series at the hourly scale, thus requiring to be adapted with respect to the original SDM (Switanek et al., 2017). The correction is applied independently at each EURO-CORDEX grid cell and separately for each calendar month. Hourly values lower than 0.1 mm/h are treated as dry hours, while positive values are adjusted assuming a lognormal distribution, selected as a parsimonious option for non-negative and strongly right-skewed hourly rainfall amounts. The original SDM rain-day frequency correction was adapted by replacing rain days with wet hours: when the target wet-hour count is lower than the modelled count, the smallest wet-hour amounts are set to zero, thus minimally affecting total accumulation, whereas when it is higher, the largest values immediately below the 0.1 mm/h threshold are reclassified as wet and intensity-corrected until the target count is reached. The use of a parametric CDFs also allows values exceeding the historical range to be adjusted through extrapolation of the fitted distribution. The time series of daily maximum and minimum temperatures are corrected, following the same procedure proposed in Switanek et al. (2017), with the detrending procedure and then using a normal distribution as the parametric distribution.

As a reminder, hourly ground precipitation measurements and E-OBS daily maximum and minimum temperatures are used as reference meteorological variables. Since the bias-correction is applied at the RCM-GCM grid scale, the reference historical variables are interpolated over the EURO-CORDEX EUR−11 grid. Moreover, as explained above, hourly precipitation observations cover the period 1995–2010, while daily maximum and minimum temperature observations cover the period 1981–2010; these two time-spans are respectively assumed as calibration periods for bias correction of the two variables.

Bias corrected (BC) time series are presented in the following sub-section considering different time periods: specifically, 1981–2010 as the reference for current conditions while the 3-decades periods 2011–2040, 2041–2070, and 2071–2100 as indicative for future conditions for near, medium, and long-time horizons, respectively. It should be emphasized that the aforementioned approach is solely limited to univariate corrections, neglecting the consideration of spatio-temporal correlations and the complex topic of downscaling. Such a constraint is acknowledged in the literature, where the challenges of incorporating spatial and temporal dependencies are well-documented (e.g., Vrac and Friederichs, 2015). Similarly, downscaling is recognized for its complexity and the potential for introducing biases if not properly addressed (Maraun and Widmann, 2018). In this sense, the hourly SDM implementation should be interpreted as a pragmatic adaptation of a climate-signal-preserving bias-correction method to sub-daily precipitation. Its adequacy is assessed in Section S2 of the Supplement through wet-hour frequency, hourly precipitation quantiles and multi-hour

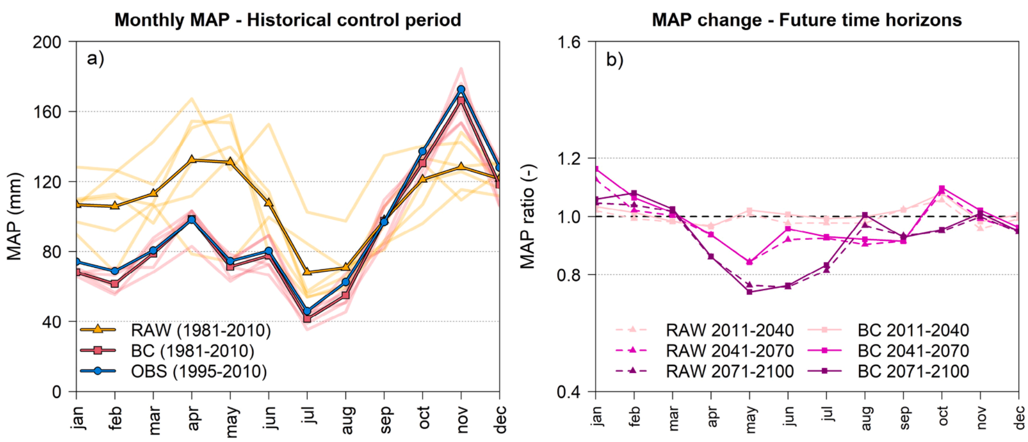

Fig. 2. Monthly mean areal precipitation (MAP). Panel a) average values in the reference control period: blue line refers to observations (OBS), bolder yellow line to the RAW models ensemble mean, bolder red line to the BC model ensemble mean, light shaded lines to single climate models; panel b) expected change of the ensemble monthly average precipitation in different time horizons in respect to the historical period. Dotted lines with triangular points and solid lines with squared points refer respectively to RAW and BC ensembles.

precipitation maxima.

4.3. Effectiveness of bias-correction and expected changes in future meteorological forcings

The results of the bias-correction procedure are reported in this section, considering the climatic models as an ensemble. Thus, we will refer to monthly (or seasonal) model output statistics averaged over the six considered models (i.e. RAW and BC ensemble mean). Here, we will always refer to the mean areal outputs, i.e. spatially averaged over the entire Panaro basin. The validation of the bias-correction accuracy at the RCM grid-scale is reported in the Supplement (Section S2).

4.3.1. Precipitation

Fig. 2a displays the results of the bias-correction procedure on the study catchment in the reference control period 1981–2010 for the long-term mean areal precipitation (MAP), cumulated at monthly scale, obtained on the basis of respectively the gauge observations (OBS, blue line), and the raw (RAW, yellow lines) and bias-corrected (BC, red lines) simulations. While shaded yellow and red lines refer to the six single climate models, the bolder solid lines refer to their ensemble averages. The added value resulting from the adoption of the bias correction in terms of cumulative monthly values is evident: the seasonal pattern of raw simulation, strongly biased, is re-aligned to observations. For some of the bias-corrected climate chains, small differences from observations remain.

Fig. 2b reports instead the ensemble climate change signal (anomaly) for monthly MAP, i.e. the expected changes in the near, medium and long-time horizons with respect to the current climate for both raw and bias-corrected simulations. In particular, it shows the average (over the six models of the ensemble) of the ratio between the MAPs projected for each of the three future time-windows and the corresponding MAP simulated in the control period, respectively for RAW and BC series. It can be seen that the climate change signal identified by raw models over the future decades is preserved in BC simulations due to the nature of the SDM bias-correction technique. The most significant future changes are mainly in the spring and summer months, which are expected to be increasingly drier throughout the decades, with precipitation depths decreasing as far as 20% for the farthest horizon (2071–2100). Autumn months are also interested by a decrease in rainfall amount starting from the half of the century, even if less pronounced.

Since the present study focuses on the simulation of past and future flood events, in addition to the monthly values, the extreme precipitation values are also investigated. Keeping into consideration the estimated response time of the catchment, the 24-hours cumulated rainfall is assumed to be representative of the flood generation processes and the maximum 24-hours rainfall depths occurring in each season are computed. Fig. 3a reports the average (over all the reference years) of the seasonal maximum 24-h MAP simulated by the six models of the ensemble. In general, the correction (red squares) tends to underestimate the observed maximum areal rainfall (blue circles), but the procedure is still able to bring the values closer to the observed ones in respect to the raw data, except for the winter season where the correction underestimates even more than the raw models.

The expected pattern of future maximum rainfall events is reported in Fig. 3, where panel b) reports the results for raw simulations and panel c) for the bias-corrected ones. The future anomaly is here expressed as the ratio between the RAW (panel b) or BC (panel c) maximum 24 h MAPs projected for each of the three time-horizons and the corresponding values simulated by the same RAW (or BC) chain in the control period. In general, maximum rainfall seems to moderately increase along the decades in the cold seasons (DJF and SON), remaining stable in spring and highly fluctuating in summer. In addition, the expected changes in maximum rainfall are well-preserved by the SDM procedure.

4.3.2. Temperature

Fig. 4a shows the results of the bias-correction procedure in the reference control period 1981–2010 for the mean areal maximum daily temperature (MAT max, but the results for MAT min are similar), with the same marker and colour meanings applied for the

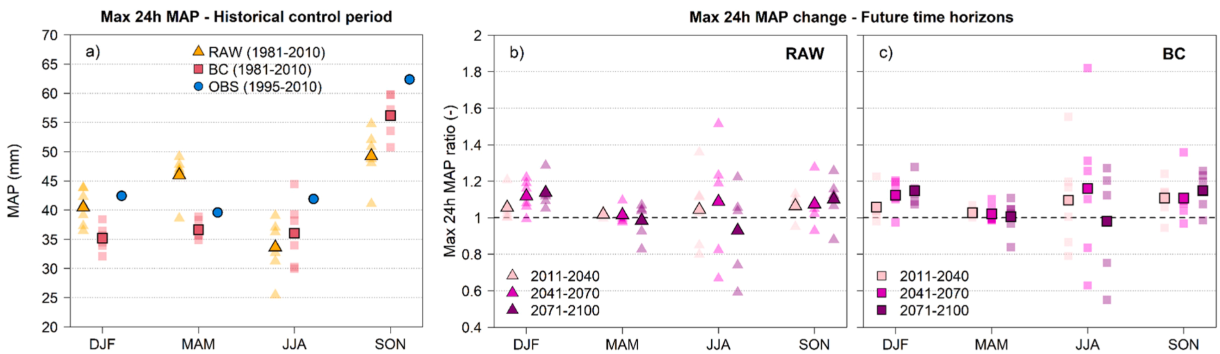

Fig. 3. Panel a) Seasonal maximum 24 h MAP (averaged over the years) in the reference control period: blue dots refer to observations (OBS), bolder orange dots to the RAW models ensemble mean, bolder red dots to the BC model ensemble mean, light shaded dots to single climate models. Panel b) and c) change of seasonal average maximum 24 h MAP simulated by RAW and BC models, respectively, expressed as the ratio between the maximum 24 h MAP expected in the future periods and the 24 h MAP simulated for the control period. Bolder dots refer to the ensemble mean, light-shaded dots to single climate models. DJF, MAM, JJA and SON refer to winter, spring, summer and autumn seasons.

mean areal precipitation graphs. In general, even if raw models already capture the temperature seasonal pattern well, the bias adjustment significantly improves the results for all the months and models.

Fig. 4b reports instead the ensemble climate change signal (also called anomaly) for MAT max in terms of expected changes in the ensemble monthly average temperatures in the near, medium and long-time horizons in respect to the current climate. First, it can be seen that the climate change signal projected by raw models over the future decades is preserved in BC simulations, as expected, due to the nature of the SDM bias-correction technique. In terms of the magnitude of the change, temperatures are expected to increase all-over the year but especially in the spring and summer months and progressively in future decades, up to 4/5 °C in the long-time horizon.

5. Streamflow simulation for the assessment of past and future flood volumes

In the present study, the actual purpose of the bias-correction analysis is to provide climatic input to rainfall-runoff models for the past and future streamflow simulation, thus providing a reliable climatic-hydrological modelling coupling. Before that, it is essential to assess the capability of the raw and bias corrected scenarios to provide meteorological fields that are consistent with the hydrological response over the study basin during the control (historical) period, with a special focus on the frequency and magnitude of floods.

To this aim, in the following phase of the validation methodology, rainfall-runoff models are used to simulate the streamflow at the basin outlet when fed respectively with the observed fields and the raw and bias-corrected climate scenarios, verifying the effectiveness of the bias-correction approach in regard to the reproduction of the streamflow regime over the past years.

As anticipated previously, in order to exclude the dependency of the outcomes on a specific model structure, the approach is tested by using two conceptually different hydrological models: the semi-distributed TUW model and the lumped Cemaneige-GR4H model.

First, the two models are parameterised, providing as input the observed fields during the historical period for which hourly streamflow records are available at the basin outlet. Calibrated models are then used to simulate streamflow in the control period when forced either with observed fields, raw climate scenarios, or bias-corrected climate scenarios. Finally, rainfall-runoff models are fed with the projected meteorological fields of raw and bias-corrected climate scenarios in future decades.

5.1. *Rainfall-runoff models and model runs*

The *TUW model* is a semi-distributed version of the HBV model (Bergström, 1976; Lindström et al., 1997) developed by Viglione and Parajka (2018). It consists of a snow module, a soil moisture module and a flow response and routing module. The model processes the sub-basins as autonomous entities that contribute separately to the total outlet flow. The inputs are hourly air temperature, precipitation and potential evapotranspiration over the different elevation zones. Finally, the different outputs from the elevation zones are averaged based on the sub-catchment areas.

In this study, the model is run with the semi-distributed model structure obtained by dividing it into 200-meters elevation zones. While model inputs and model states are defined over such zones, model parameters are assumed to be the same for the entire catchment. In the configuration used here, 13 out of the total 15 parameters are calibrated.

The second model is the French *CemaNeige-GR4H* (Coron et al., 2017). It is the combination of the CemaNeige snow accounting routine (Valéry et al., 2014) with the GR4H model (Mathevet, 2005), a hourly lumped continuous rainfall-runoff model, developed at INRAE (Antony, France), by the Équipe Hydrologie des Bassins versants. The inputs of the model are spatially-averaged catchment hourly air temperature, precipitation and potential evapotranspiration. The model is governed by 6 parameters, to be calibrated. For

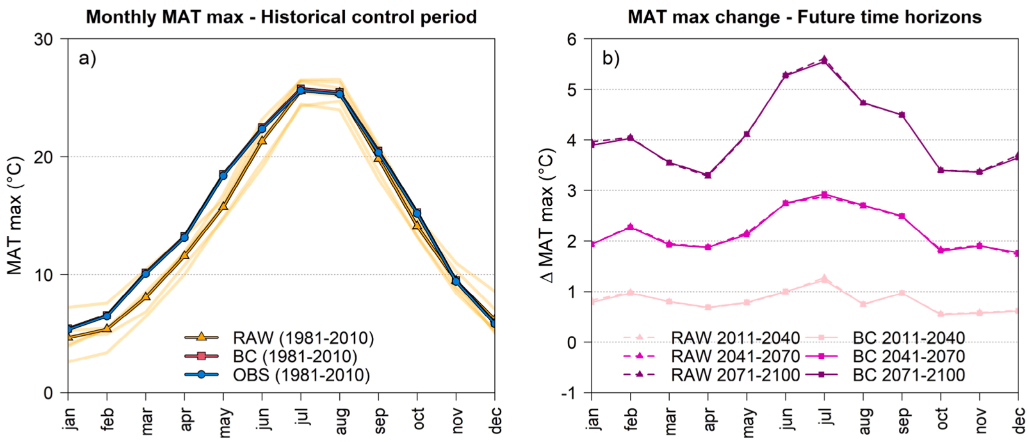

Fig. 4. Mean areal maximum daily temperature (MAT max). Panel a) average monthly values in the reference control period: blue line refers to E-OBS, orange line to the RAW models ensemble mean, red line to the BC model ensemble mean, light shaded lines to single climate models; panel b) future change of the ensemble monthly average temperatures in future decades in respect to the control period simulations. Dotted lines with triangular points and solid lines with squared points refer respectively to RAW and BC ensembles.

the sake of brevity, we will refer to this model just with the acronym GR4H, even if it will always include the CemaNeige snow module.

For both models, potential evapotranspiration is derived from temperature time series using the simplified method proposed by Blaney and Criddle (1962). More details about model routines and parameters are given in the Supplement (Section S3).

The parameterisation of the models is performed by forcing them with observed meteorological input and minimising the differences between the simulated outputs and the observed records of hourly discharges, available at the basin outlet during the period 2007–2015. For the sake of brevity, a detailed description of model parametrisation and their calibration performances are reported in the Supplement (Section S4). Overall, the performances are satisfactory and both rainfall-runoff models behave well: Kling–Gupta efficiencies is 0.882 for TUW and 0.865 for the GR4H model, while Nash Sutcliffe efficiency is 0.729 for TUW and 0.725 for the GR4H model.

Once the models are parameterised, they can be used to simulate streamflow at basin output by forcing them with different inputs over the past and future decades. Depending on the type of meteorological fields used to force models, the hydrological simulations will be here denoted as:

- *TUW-obs* and *GR4H-obs* when the models are forced with observed meteorological fields. In this case, hourly precipitation and temperature are the same defined to calibrate the models. According to climatic inputs availability, the models can be run from 1995 to 2010. Given the obtained calibration performances, such simulations are assumed to be representative of the streamflow regime at the basin output.
- *TUW-raw/bc* and *GR4H-raw/bc* when the models are forced with meteorological fields simulated by one of the raw/bias-corrected EURO-CORDEX scenarios. Hourly precipitation is directly spatially averaged from CORDEX domain, assigning weights to each cell based on the portions of the basin (or elevation zone) area covered by each of them. Hourly temperature is instead computed from the hourly interpolation on the 24 h of maximum and minimum CORDEX temperatures as done for E-OBS estimates, then spatially averaged. Such model simulations (raw and bias-corrected) are run from 1981 to 2100.

5.2. *Effectiveness of the bias-correction approach on streamflow modelling in the control period*

The core objective of the experiment is to evaluate the effectiveness of the bias-correction approach, applied to raw hourly climate scenarios, for the reproduction of the streamflow and for the simulation of flood events. As previously mentioned, the flood volume is of particular interest for the design and operation of the flood retention systems in the study catchment and in the region, which would be considerably more affected by a future increase in flood volumes rather than in flow peaks.

The simulations obtained by forcing the rainfall-runoff models with the raw and bias-corrected modelling chains (TUW-raw/bc and GR4H-raw/bc) are compared to those obtained by using the input derived from historical meteorological observations (TUW-obs and GR4H-obs) during the historical control period.

The comparison is performed by considering both the streamflow seasonality and the frequency and magnitude of flood events. Analogously to what was done for precipitation and temperatures series (4.3), the selected streamflow features are computed comparing the TUW-raw/bc and GR4H-raw/bc simulations over the entire control period 1981–2010 to those retrieved from for TUW-obs and GR4H-obs simulations in the shorter observation period 1995–2010. The first year of each simulation is always used as warm-up and thus excluded.

5.2.1. *Seasonal streamflow regime in the historical period*

Fig. 5 compares, for TUW (panel a) and GR4H (panel b) models respectively, the annual cycle of discharge (multiyear regime of 30-

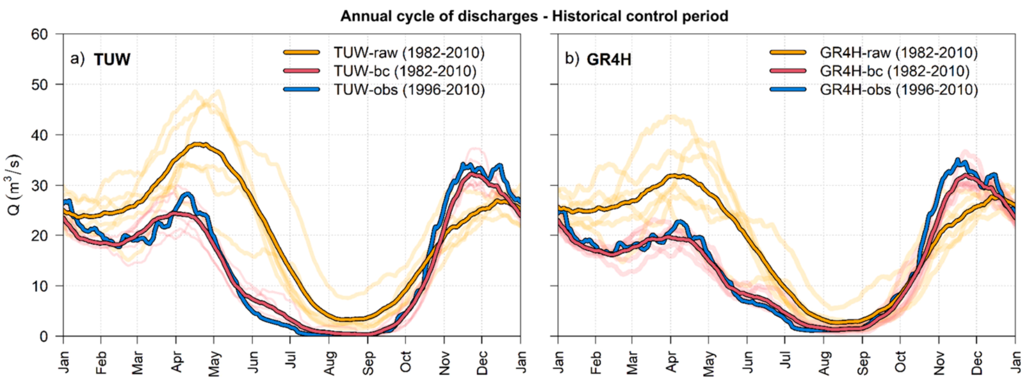

Fig. 5. Annual cycle of discharges in terms of multiyear regime of 30-days averaged flows in the historical control period for TUW (panel a) and GR4H (panel b). Blue lines refer to the simulations obtained with observed meteorological forcings (TUW-obs and GR4H-obs), bolder orange lines to the ensemble average of the simulations obtained with RAW climatic forcings (TUW-raw and GR4H-raw), bolder red lines to the ensemble average of the simulations obtained with BC climatic forcings (TUW-bc and GR4H-bc). Light shaded lines refer to the simulations obtained by forcing hydrological models with single climatic chains.

days averaged flows) obtained by running the models with observed inputs (blue) against those simulated using as forcing variables the raw (orange) and bias-corrected (red) climate scenarios during the historical period of reference.

First, it can be noticed how the results are in line for the two rainfall-runoff models. As expected and consistently to what observed for the pattern of monthly MAP (Fig. 2a), the simulations forced by raw climate scenarios (TUW-raw and GR4H-raw) show in general an overestimation of discharges during most of the year, with the exception of autumn months where the flow is slightly underestimated. On the other hand, when feeding rainfall-runoff models with bias-corrected forcings (TUW-bc and GR4H-bc), the seasonality of the ensemble mean monthly discharges is generally realigned to those of TUW-obs and GR4H-obs.

5.2.2. Frequency, peaks and volumes of flood events in the historical period

Once verified that the bias-correction approach is overall able to adjust the seasonality of monthly streamflow, the reliability of the approach to simulate high flows and flood events is investigated. In particular, flood events are identified from the simulated discharge time series adopting the peak over threshold (POT) approach (e.g. Lang et al., 1999; Poncet et al., 2024), which consists of the extraction of all the flood peaks exceeding a threshold. Here, such threshold is set to the 95th quantile of observed discharge (as done e.g. by Viglione et al., 2013). In addition, since the POT method assumes temporal independence between flood peaks, a declustering algorithm - adapted from Lang et al. (1999) - is implemented to identify and separate dependent events. In this study, two flood peaks are considered independent if they are separated by at least 96 h and if the intervening discharge drops below 75% of the lower of the two peak values.

The features of the flood events (with peaks overpassing the 95% threshold) identified on the historical period are analysed both at annual and at seasonal scale. Specifically, three metrics are considered:

- flood occurrence F_{95} (-), expressed as the number of events per year/season;
- peak over threshold magnitude POT_{95} (m^3/s);
- flood volume over threshold VOT_{95} (m^3), i.e. the hydrograph volume above the fixed threshold.

Fig. 6 shows the cumulative distribution functions (CDFs) of the POT_{95} of the events identified in the TUW simulations over the historical control period: the CDFs obtained from the TUW-obs simulation (blue) are compared to the TUW-raw curves in the upper panels, and to the TUW-bc (red) curves in the lower panels. The CDFs on the left (panels a and e) include the events occurring in anytime along the year, while the CDFs in the other panels focus on winter (DJF), spring (MAM) and autumn (SON) events exclusively. Summer events are excluded from the CDF plots as their low frequency does not allow for a meaningful statistical characterization. Fig. 7 shows instead, with the same fashion, the cumulative distribution function of VOT_{95} over the historical control period for TUW model. Similar considerations can be made for POT_{95} and VOT_{95}: overall, looking at the CDFs of the events occurring across the entire year, raw simulations (panels a in both Figs. 6 and 7) appear to well reproduce peak and volume distributions. However, when focusing on the different seasons, the CDFs of TUW-raw deviate substantially from those of TUW-obs in spring (MAM, panel c), where most intense floods are overestimated, and especially in autumn (SON, panel d), where all floods are instead generally underestimated. On the other hand, TUW-bc simulations (red, lower panels) are able to realign the seasonal CDFs with the observation-based runs. Since POT_{95} and VOT_{95} distributions of GR4H model are very similar, they are reported in the Supplement only (Section S5) for the sake of

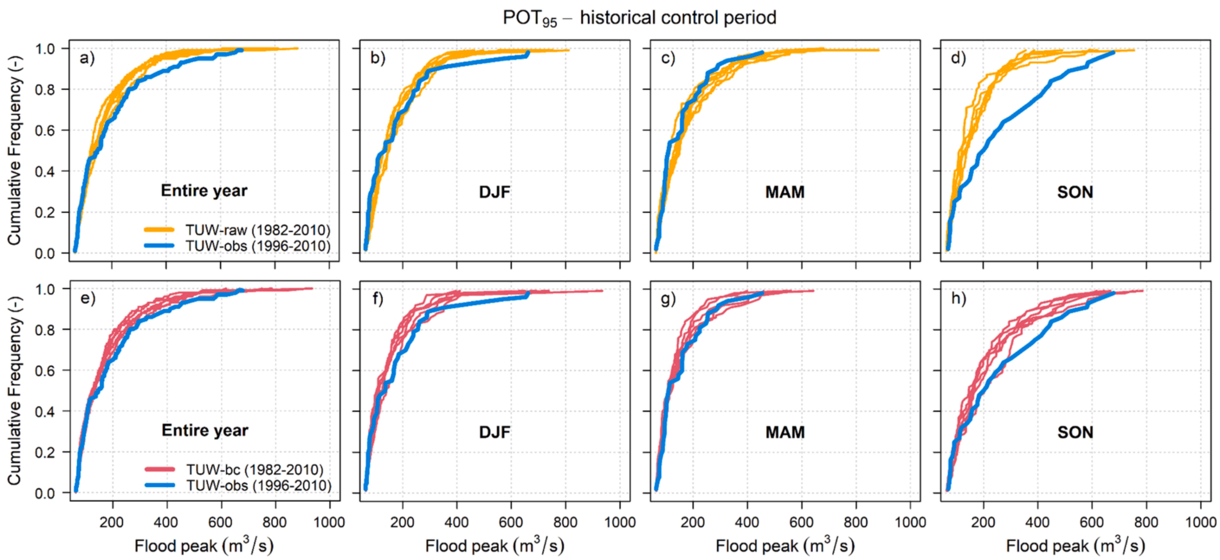

Fig. 6. Cumulative distribution functions (CDFs) of POT_{95} over the historical control period for the TUW-raw (orange, upper panels) and TUW-bc (red, lower panels), against TUW-obs (blue) runs. CDFs of panels a and e refer to all the events across the year, while panels b to d and f to h refer respectively to winter (DJF), spring (MAM) and autumn (SON) events.

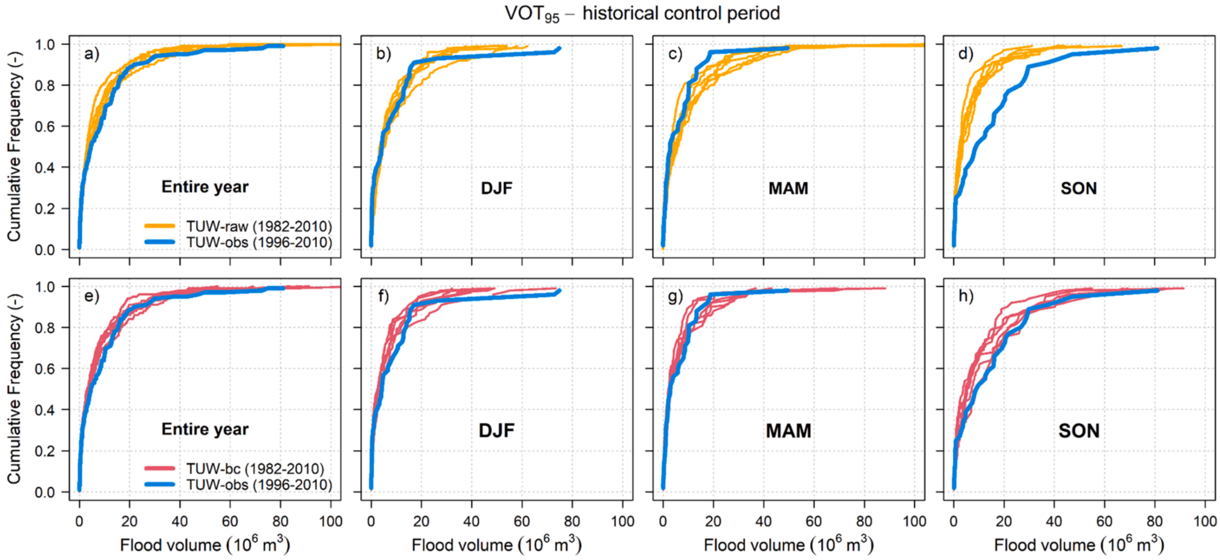

Fig. 7. Cumulative distribution functions (CDFs) of VOT_{95} over the historical control period for the TUW-raw (orange, upper panels) and TUW-bc (red, lower panels), against TUW-obs (blue) runs. CDFs of panels a and e refer to all the events across the year, while panels b to d and f to h refer respectively to winter (DJF), spring (MAM) and autumn (SON) events.

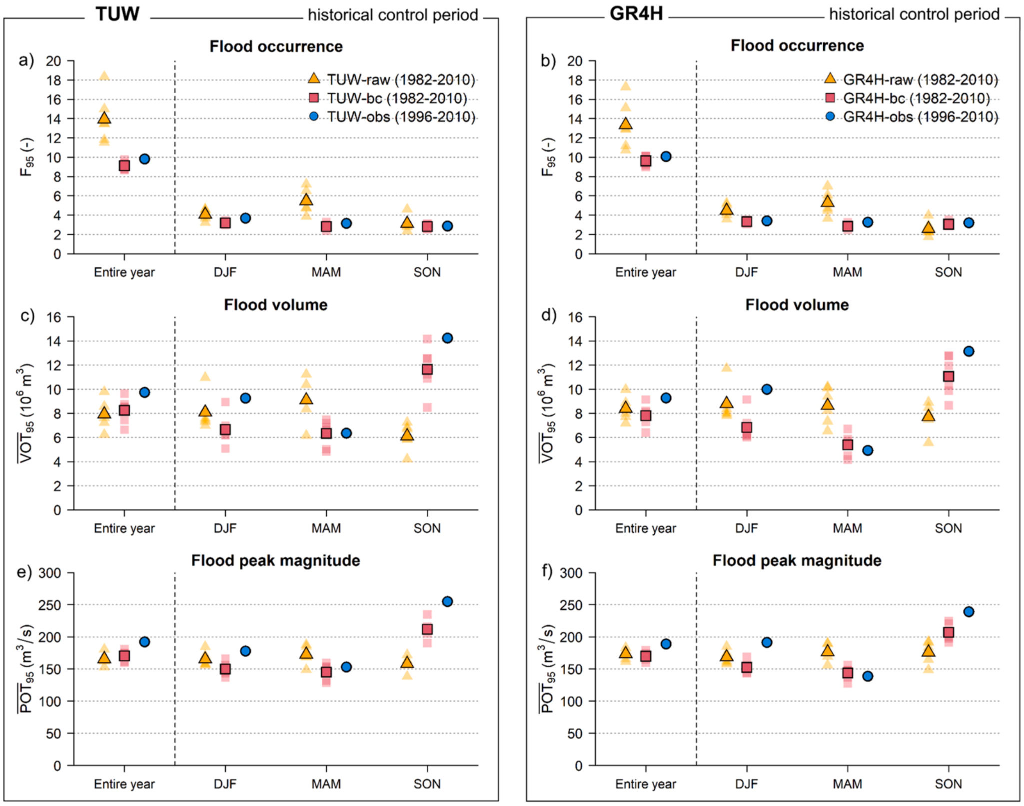

Fig. 8. Flood event metrics in the historical control period: average flood frequency (n° events per year F_{95}, panels a and b), average flood volume ($\overline{VOT}_{95}$, panels c and d) and average flood peak magnitude ($\overline{POT}_{95}$, panels e and f) for the TUW model (left) and GR4H model (right) respectively. Blue dots refer to TUW-obs, bolder orange dots to the TUW-raw and GR4H-raw ensemble mean, bolder red dots to the TUW-bc and GR4H-bc ensemble mean, light shaded dots to the average statistics of single climate models. DJF, MAM and SON refer to winter, spring and autumn seasons.

brevity.

In order to better validate the effectiveness of the modelling chain for the reproduction of flood events characteristics, average flood metrics in the control period are also shown. Fig. 8 shows average flood frequency (number of events per year/season) and the corresponding average peaks, POT_{95}, and volumes. VOT_{95}, in the historical period, both at annual and seasonal scale (again, statistics of the very few summer events are excluded). The outcomes are consistent between the two hydrological models. For what concerns the frequency of flood events (panels a and b), the bias-correction is definitely able to properly adjust the average number of events per year to the simulation forced with meteorological observations, both at annual and seasonal scale (whereas the number of events is overall overestimated throughout the years by raw simulations). When analysing the average volume (panels c and d) and average peak (panels e and f) of the flood events, the benefit of the bias correction is evident by its ability to reduce the overestimation in spring and the underestimation in autumn (that, when taken together over the entire year, balance out each other), while for the winter season the corrected models underestimate even more than the raw models.

5.3. Expected changes in future flood regime

The analysis of the previous section verified that the proposed bias-correction approach is able to properly adjust hourly climate model outputs, not only to faithfully reproduce past historical climate, but also to produce reliable streamflow simulation when they are used to force the selected rainfall-runoff models.

The last step of the approach is the evaluation of future changes in flood regime. Only the simulations produced by forcing the hydrological models with bias-corrected scenarios (TUW-bc and GR4H-bc) are considered here. Similarly to what done for climatic outputs, since the bias-correction is applied separately over the three different 30 years-time horizons (see 4.2), the evaluation of the expected changes in flood regime is analysed accordingly.

Before looking at the future evolution of the flood events, the expected change in the seasonal flow regime is assessed. Fig. 9 shows the ensemble 30-days averaged flows obtained in the control period (grey lines), compared to ensemble averages projected for the future time horizons: 2011–2040, 2041–2070 and 2071–2100 (pink, magenta and violet lines respectively). While no substantial changes are projected in January and Febraury, long-term average flow is expected to decrease from March to June, progressively during the coming decades. In November and December instead, the ensemble shows a decrease exclusively for the farthest time horizon (2071–2100).

Fig. 10 reports the expected changes in flood event metrics, simulated by TUW-bc (left) and GR4H-bc (right). The outcomes are here analysed by comparing them to the expected changes in maximum 24 h precipitation (Fig. 3c), but also to the evolution of the long-term annual flow cycle (Fig. 9), which represents a proxy of the average basin moisture state when high rainfall events occur. Overall, the results, which are consistent between the two models, show us that the selected model ensemble is projecting a reduction in the occurrence of flood events across the entire year, together with an intensification of their magnitude, in terms of both flood volume and peak. Again, the analysis of the evolution of flood dynamics at seasonal scale better supports the interpretation of such outcomes.

The frequency of flood events (panels a and b) in autumn (SON) and spring (MAM) is expected to decrease in the coming decades. On the other end, the expected pattern of winter (DJF) flood occurrences is less clear, with a very slight increase only in the first two time-horizons and a wide spread of the ensemble at the end of the century.

Peaks and volumes of flood events are predicted to experience a similar future evolution. Considering the entire year, the average peaks, POT_{95}, and volumes, VOT_{95}, are increasing, and this is mainly due to the autumn events. In the other seasons, instead, the intensification of flood magnitude is very limited.

The outcomes of this analysis highlight that the expected changes in future flood dynamics within the study basin are influenced by multiple factors depending on the season, which will be discussed further below.

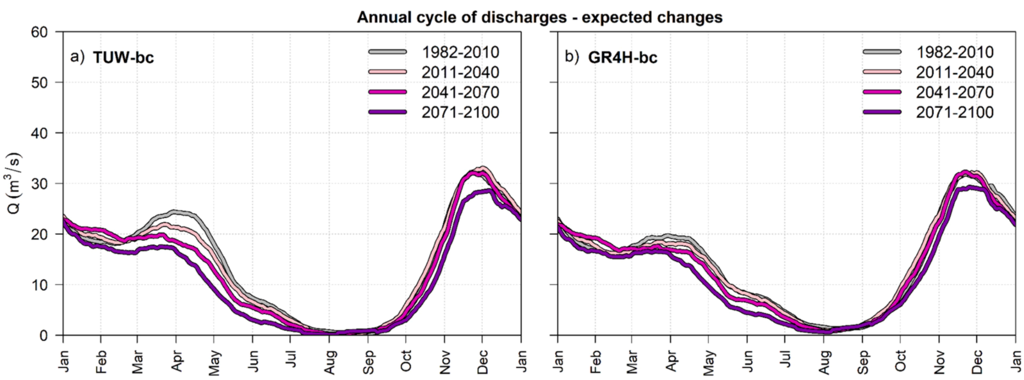

Fig. 9. Future expected changes in the annual cycle of discharges in terms of multiyear regime of 30-days averaged flows for TUW-bc (panel a) and GR4H-bc (panel b). Lines refer to ensemble average simulation obtained with BC climatic forcings over the future time horizons (pink, magenta and violet) compared to the ensemble historical simulation (grey).

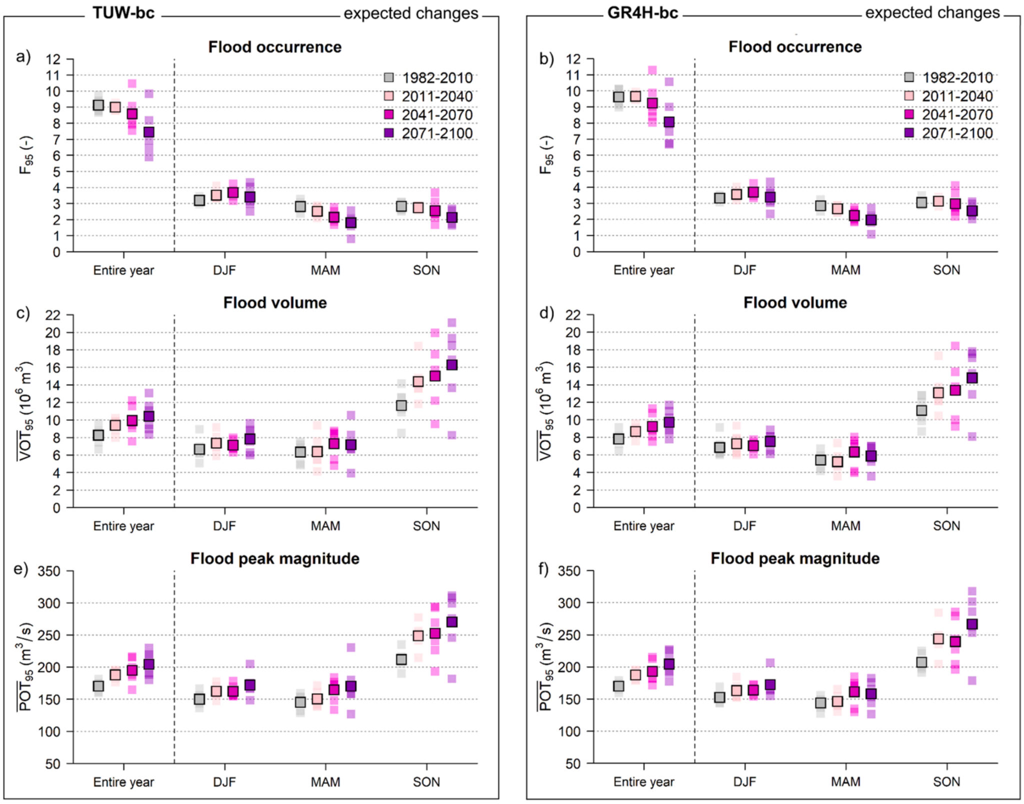

Fig. 10. Future expected changes in flood event metrics: average flood occurrence (n° events per year F_{95}, panels a and b), average flood volume ($\overline{VOT}_{95}$, panels c and d) and average flood peak magnitude ($\overline{POT}_{95}$, panels e and f) for TUW-bc model (left) and GR4H-bc model (right) respectively. Bolder dots refer to ensemble average simulation obtained with BC climatic forcings, light shaded dots to the average statistics of single climate models. DJF, MAM and SON refer to winter, spring and autumn seasons.

6. Compound flood-on-drought events

The last step of the methodology entails the assessment of the expected changes in the temporal occurrence and magnitude of coupled drought and flood periods. As already mentioned, such analysis is motivated by multiple factors. While in general, future changes in the co-occurrence of droughts and floods are expected (e.g. Rashid and Wahl, 2022), the number of studies in the literature addressing the evolution of abrupt changes in the hydrological state is still limited (Brunner, 2023).

Here, following the same rationale of the previous phases of the work, the characterization of flood-on-drought occurrences is performed. In particular, floods occurring during droughts (identified by means of the Standardised Streamflow Index, SSI, Vicente-Serrano et al., 2012) are labelled as flood-on-drought events. Although the proposed methodology combines two widely established metrics—the POT approach for flood identification and the SSI for hydrological droughts—it introduces a novel perspective, as previous research on these compound events has predominantly relied on non-standardised drought indicators (e.g. Götte and Brunner, 2024; Matanó et al., 2024). Testing the efficacy of the SSI for this specific purpose is particularly relevant: not only does it capture the cumulative nature of water deficits over time, but it is also a widely recognized tool employed for drought monitoring and for assessing the impacts of water scarcity on agriculture and overall water availability.

The experiment showed in this section is conducted exclusively for streamflow time series (TUW-bc and GR4H-bc) obtained forcing the two rainfall-runoff models with bias-corrected meteorological time series.

6.1. SSI computation and identification of drought events

The Standardised Streamflow Index (SSI, Vicente-Serrano et al., 2012), one of the most widely used drought indexes, is adopted to detect and characterize hydrological drought events in the study catchment. The SSI is a statistical monthly indicator based on the cumulated averaged streamflow across a period of n months: the index compares the difference of such quantity, over a given time interval, with the long-term streamflow distribution for the same location and accumulation period. The calculation procedure of SSI involves two steps: fitting a probability distribution to the n-months time series of cumulated streamflow average and then transforming the cumulative probability of the fitted distribution into a standard normal distribution (with mean zero and unit variance).

Following few preliminary tests and recommendations from past studies (Lema et al., 2025; Tijdeman et al., 2020; Vicente-Serrano et al., 2012), here we use the generalized logistic distribution to compute the SSI. For the purpose of this application, an aggregation time scale of three months (i.e. SSI−3) is used, in accordance with the seasonal nature of the analysis.

SSI computation is performed for each of the simulated TUW-bc and GR4H-bc streamflow time-series, when forced with each of the bias-corrected GCM-RCM modelling chain. Similarly to what done in a number of previous studies (e.g. Osuch et al., 2016; Spinoni et al., 2020, 2015), we selected the entire period (1981–2100) as a baseline period to fit the underlying probability distributions of the drought indicator, so that the 3-months averaged streamflow thresholds used for identifying a drought (see below) do not change along the entire century.

Once we had computed the SSI−3 values for each month from 1982 to 2100, we identified the drought by means of the "run theory'' as proposed by Yevjevich (1967). That is to say: a drought starts when the drought indicator falls below one negative standard deviation for at least two consecutive months and ends when the indicator turns positive.

Fig. 11 illustrates the evolution of drought characteristics across the future time horizons. In particular, it shows the total drought duration (i.e. the "months in drought"), expressed as the n° of months belonging to drought events in a 30-years period (panel a), the average duration of drought events (panel b) and the average severity of the events, expressed as the sum of SSI absolute values during the drought (panel c). It can be noticed that drought statistics simulated by the two rainfall-runoff models are consistent between each other, and for both models the hydrological droughts in the region are projected to become progressively longer and more severe towards the end of the century.

6.2. *Expected changes in flood-on-drought events*

Once SSI-based droughts have been detected, the subset of flood events occurring during such periods (flood-on-drought events) are identified and their evolution along the entire century is investigated.

The same three indicators considered for overall flood events are defined for such compound events: flood-on-drought occurrences F_{FonD} (-), expressed as the number of events per year/season), the average flood-on-drought peak magnitude $\overline{POT}_{FonD}$ (m^3/s), and the average flood-on-drought volume $\overline{VOT}_{FonD}$ (m^3).

The results of the experiment are reported in Fig. 12, following the same format adopted in the previous section when considering all the flood events. On an annual basis, despite the overall decrease in the frequency of all the flood events (F_{95}, Fig. 10a-b), the occurrence of flood-on-drought ones (F_{FonD}, Fig. 12a-b) clearly shows a significant opposite upward future trend in the coming decades, with a projection of a triple number of these types of events by the end of the century according to both rainfall-runoff simulations. By focusing on individual seasons, it can be observed that the largest increase in such events occurs during winter (DJF).

Comparing the magnitude (peaks and volumes) of flood-on-drought events (Fig. 12) with that of all floods (Fig. 10), in terms of both average volumetric contribution (panels c and d) and average peak discharge (panels e and f), it is evident that events occurring during droughts are, on average, of lower intensity, as expected. Regarding the projected changes for such events, no significant future shift is detected. In particular, the variability of the two metrics across simulations forced by different GCM-RCMs is very high and does not result in a clear future signal.

7. Discussion

A comprehensive interpretation of the findings requires assessing the cascading impacts of the bias correction procedure on hydrological simulations, alongside the expected future changes in hydrometeorological extremes and flood dynamics.

The results highlight that the application of a bias correction (BC) procedure was absolutely necessary, particularly for precipitation. The uncorrected (raw) climate models exhibited a significantly distorted seasonality in terms of both mean and extreme rainfall when compared to ground observations. Overall, the BC procedure successfully mitigated these discrepancies, effectively realigning the modelled climate dynamics with the observed regime.

Regarding the annual cycle of precipitation (Fig. 2a), minor differences between some bias-corrected climate chains and the observations persist. These residual discrepancies can likely be attributed to the fact that observational data are available for only a part

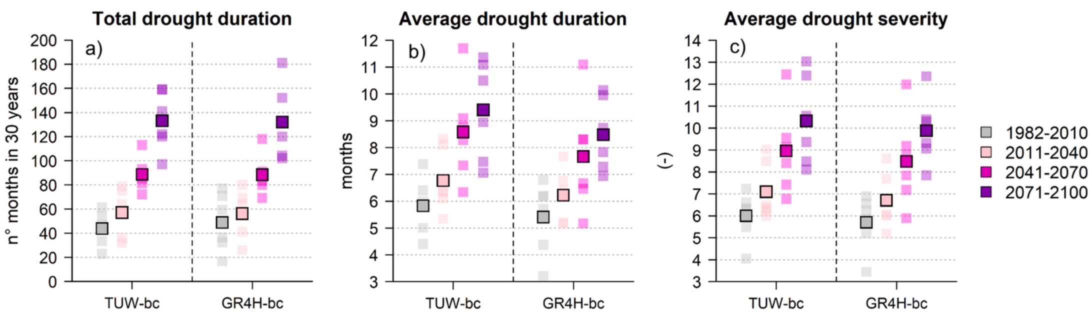

Fig. 11. Future pattern of drought characteristics: a) total drought duration, expressed as the n° of months belonging to drought events in a 30-years period; b) average duration of drought events; c) average severity of the events, expressed as the sum of SSI absolute values during the drought.

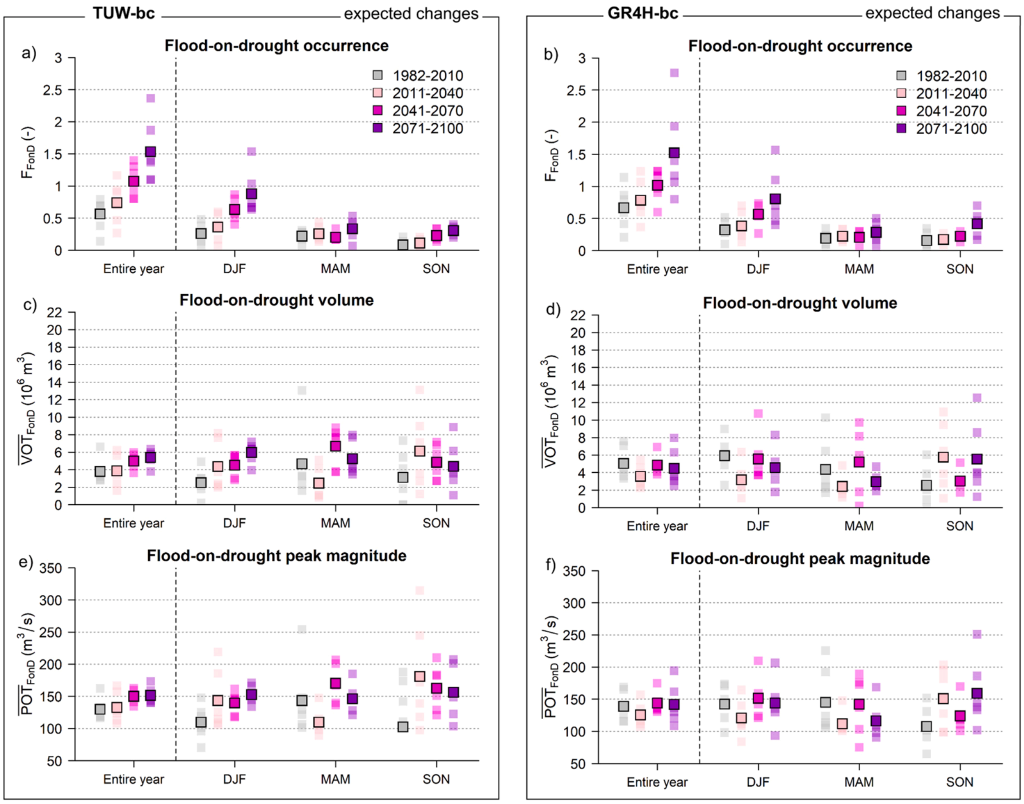

Fig. 12. Future expected changes in flood-on-drought event metrics: average flood-on-drought occurrence (n° events per year F_{FonD}, panels a and b), average flood-on-drought volume ($\overline{VOT}_{FonD}$, panels c and d) and average flood-on-drought peak magnitude ($\overline{POT}_{FonD}$, panels e and f) for TUW-bc model (left) and GR4H-bc model (right) respectively. Bolder dots refer to ensemble average simulation obtained with BC climatic forcings, light shaded dots to the average statistics of single climate models. DJF, MAM and SON refer to winter, spring and autumn seasons.

of the years (1995–2010) constituting the historical control period (1981–2010); consequently, the inter-annual variability of the observations is thus not fully represented.

When focusing on extreme events (Fig. 3a), the effectiveness of the BC procedure on the maximum 24-hour precipitation is, unsurprisingly, lower than its performance in correcting monthly averages. This limitation primarily stems from two factors. First, maximum rainfall is not explicitly included as a variable for scaling in the SDM technique. Second, because the BC is applied independently on each grid cell, it does not explicitly impose to respect the high spatio-temporal correlation of rainfall events. As a result, the correction tends to underestimate the observed maximum areal rainfall. This behaviour was expected, since the bias-adjustment procedure has greater difficulty in correcting extreme values compared to average values (as seen in Fig. 2), as well as an even more amplified difficulty in correcting the structure of the 24-hour rainfall events compared to the single hourly data. Despite these limitations, the BC procedure consistently brings the simulated extreme values closer to the observations compared to the raw models.

The performance of the BC on precipitation fields cascades directly into the hydrological responses simulated by the two rainfall-runoff models. The BC procedure successfully adjusts the seasonality of both the mean annual streamflow cycle (as depicted by the 30-day moving window in Fig. 5) and, most importantly for the present study, the flood events in terms of peaks and volumes. While their Cumulative Distribution Functions (CDFs, see Figs. 6 and 7) at the annual scale show similar curves with minimal discrepancies between raw and corrected inputs, analyzing the data at the seasonal scale reveals the crucial value of the BC. More in particular, comparing the magnitude of flood volumes and peaks (Fig. 8) with the pattern of maximum 24 h precipitation (Fig. 3a), it can be noticed that TUW-bc and GR4H-bc underestimate flood volumes in wetter seasons (DJF and SON), in accordance with the largest bias between BC and OBS precipitation extremes. In such months in fact, seasonal precipitation is higher, dry spells are limited and catchment soils are likely to be saturated; therefore, hydrological dynamics are generally faster, with most of rainfall is propagated as surface and sub-surface runoff, and the underestimation in high rainfall and floods are aligned. Despite this cascading bias, the overall seasonality of the flood event features is corrected accordingly to the observation-forced simulations; such results are consistent with those obtained by Reszler et al., (2018), who tested the effectiveness of the SDM technique on regional climate simulations for the purpose of flood modelling: they showed that the bias-correction procedure is able to adjust flood seasonality by correcting total event rainfall amounts but, since it does not account for spatial and temporal correlation of precipitation, it may also affect the dynamics of spatially extensive and persistent meteorological events, which typically trigger major flood events in meso-scale catchments.

Moving beyond the evaluation of the bias correction procedure, the second major focus of this discussion addresses the projected changes in the basin hydrometeorological regime. As a preliminary remark, the obtained results should be interpreted considering one of the limitations of the study, namely that climate-model uncertainty is only partly represented. As detailed in 4.1, the selected climate modelling chains do not constitute a full probabilistic assessment, but are rather conditional on a specific RCA4-based high-emission ensemble. While this selected subsample provides a robust representation of GCM-driven variability—thanks to the inclusion of models with widely different Equilibrium Climate Sensitivity (ECS)—it does not account for uncertainty related to RCM structure, internal variability, convective parameterisations or alternative scenarios, which may be relevant for sub-daily precipitation and flood-generating events. From a broader regional perspective, we observe that the general projected precipitation changes in future decades are in line with previous findings (EEA, 2024; IPCC, 2023; Iturbide et al., 2022) in the Southern Europe region. While this macroscopic consistency does not overcome the uncertainties tied to the limited ensemble size at the localized catchment scale, it provides a basic verification of the overarching climatological signals: while seasonal precipitation is expected to decrease from April to July, with a drop reaching 20% at the end of the century, maximum rainfall seems to moderately increase along the decades in the cold seasons (winter and autumn), remaining stable in spring and highly fluctuating in summer.

Translating these climate signals into streamflow scenarios inherently relies on the chosen modelling chain. It is clear that one of the main advantages of the chosen parsimonious model structures is that meteorological forcings are the only input data required, thus making the methodology easily transferable to different case studies. On the other hand, they cannot, of course, account for changes other than in rainfall and temperature inputs, such as potential future changes in land use, root zone capacity, vegetation, and human interventions. Furthermore, potential evapotranspiration is estimated from temperature using the Blaney-Criddle method. This formulation was chosen due to the limited data availability—specifically, solely precipitation and temperature data—which precluded the application of more physically based, albeit still empirical, approaches like the Penman-Monteith equation. These choices are simple and highly transferable, and common to many impact studies in the literature (e.g., among many others, Chauveau et al., 2013; Lemaitre-Basset et al., 2021; Z. Li et al., 2022; Melsen et al., 2018; Poncet et al., 2024), but they undeniably represent a limitation that must be carefully taken into account when analyzing the simulated projections.

The simulated future pattern of the annual cycle of discharges (Fig. 9) is consistent with the climate change signal for future precipitation and temperatures. The already mentioned future precipitation decrease, combined with the exceptional expected temperature rise, up to 5.5 °C (twice compared to the temperature increase expected for the medium time horizon 2041–2070), implies that the basin state from mid- to late spring and at the beginning of autumn will be more likely dry, significantly affecting rainfall-runoff dynamics.

Expected changes in future flood dynamics within the study basin are influenced by multiple factors depending on the season. The frequency of flood events (Fig. 10, panels a and b) in autumn and spring is expected to decrease in the coming decades. This behaviour can be associated much more with the expected pattern of long-term average flow (Fig. 9) than with the future changes in 24 h precipitation maxima (Fig. 3c). In such seasons in fact—especially in spring where the reduction of flood occurrences in the future decades is more pronounced—the average flow, which represents an indicator of the catchment status preceding the rainfall events, is projected to be progressively lower. We verified this behaviour by analysing the basin antecedent condition before the flood events, using the simulated water content in all the internal storages within the conceptual models as its proxy, alongside the characteristics of the precipitation events that triggered the floods. This supporting analysis, detailed in Section S6 of the Supplement for the sake of brevity, supports the interpretation that the reduction in flood occurrence is linked to progressively drier antecedent conditions over the course of the century. Concurrently, the precipitation events triggering these floods are found to be more intense, compensating for the higher infiltration capacity of the basin. Notably, future drier soil moisture conditions increase infiltration processes, reduce the surface runoff generated by the successive high rainfall events, and can compensate for the increase in heavy precipitation for small to moderate floods (e.g., Bertola et al., 2021; Brunner et al., 2021; Tramblay et al., 2023; Wasko and Guo, 2022). This compensating effect is not observed in the same way during winter (DJF), where future evolution of flood occurrences is less clear, with a very slight increase only in the first two time-horizons and a wide spread of the ensemble at the end of the century. This indistinct pattern may be due to the combination of a progressive but moderate increase in winter maximum precipitation and drier antecedent catchment conditions.

On the other hand, changes in the magnitude of flood peaks and volumes are very limited for all seasons except for autumn, when the expected strong increase in the 24 h precipitation maxima (Fig. 3), likely combined with higher seasonal average flows (Fig. 9), translates into a substantial increase in flood volumes and peaks.

In general, while the intensification of extreme rainfall events in autumn is expected to lead to increased flood peaks and volumes, floods are projected to become less frequent, especially in spring, due to the overall drier long-term hydrological conditions in the watershed.

Building on these shifts in flood-generating conditions, the future evolution of flood-on-drought events reveals additional insights. Unlike the general decline projected for flood occurrences, these compound events exhibit a distinct upward trend, with their frequency expected to triple by the end of the century. This behavior is most prominent during the winter season: while floods are projected to remain overall stable in winter, the proportion of such events occurring during droughts is increasing in the future decades. In fact, while average flow conditions in winter months are expected to decrease only slightly (Fig. 9), the probability of encountering drought events—which are defined according to the season and account for the cumulative average runoff in the basin—grows as the end of the century approaches (Fig. 11). For the other seasons, instead, the overall number of flood events is expected to decrease, but since the drought condition becomes more frequent, the frequency of flood-on-drought events remains stable, with only a slight increase observed in autumn. In general, the results confirm that for the study area, and according to the metrics used in this experiment, an increase in the frequency of compound events and rapid transitions from dry periods to floods is expected, primarily driven by the increase of drought occurrences. However, similarly to what observed by larger-scale studies

(Matanó et al., 2024), these events remain, on average, of lower intensity compared to "standard" floods, and no clear evidence of their future intensification emerges from the simulations.

8. Conclusions

A methodology based on the bias-correction of hourly climate GCM-RCM simulations and continuous rainfall-runoff modelling was implemented to reproduce the occurrence and magnitude of past and future flood events in the Northern Apennines, using as a case study the mid-sized Panaro catchment. In addition to a focus on flood events, the future evolution of compound flood and drought events has also been studied, in order to obtain an estimate of the expected changes in drought-to-flood transitions.

The bias correction successfully reproduced average monthly statistics but slightly underestimated 24-hour maximum precipitation. Consequently, while the overall reproduction of flood features improved, winter and autumn flood peaks and volumes remained underestimated, reflecting the inherent limitations of the bias correction approach in capturing the spatio-temporal correlation of major rainfall events.

The analysis of the expected changes in the future flood regime highlighted that the ensemble projects a lower frequency of flood events throughout the year, especially in spring, due to the overall drier long-term hydrological conditions in the watershed, which can compensate for the increase in heavy precipitation for small to moderate floods. Yet, an increase of the flood magnitude in terms of both volume and peak is expected in autumn for the strong intensification of extreme rainfalls.

A key value of this analysis lies in its explicit focus on the seasonality of the events. Accounting for seasonal dynamics allows to highlight the crucial role of the bias-correction procedure not only in adjusting the magnitude of the forcing variables but, more importantly, in correctly realigning their timing. Indeed, the necessity of considering seasonality and anticipating changes in the seasonal regime of floods has been widely emphasized by several prominent studies (Blöschl et al., 2017; Fang et al., 2022; Gu et al., 2025)

An approach to evaluate abrupt changes from drought to flood conditions was also proposed, driven by the need for a comprehensive characterisation of compound drought and flood events, already recently raised by the hydrological community (Kreibich et al., 2019, 2021; Ward et al., 2020), who highlighted how flood or drought risk reduction measures can have (unintended) positive or negative impacts on the risk of the opposite hazard, with important implications for practical flood and drought risk management.

Overall, the authors believe that this study may provide a valuable basis to support climate adaptation strategies within the region. By estimating the expected changes in floods occurrence and magnitude, projecting the future evolution of hydrological droughts, and finally testing specific metrics for compound flood-on-drought occurrences, the research contributes to the understanding of local climatic impacts, serving as a critical foundation for informing land-protection strategies. Future work will aim to build upon this framework, primarily by using larger multi-RCM ensemble to better quantify the associated uncertainties and further strengthen the robustness of the projected scenarios, but also extending the analysis to additional Apennines catchments.

CRediT authorship contribution statement

Mattia Neri: Writing – review & editing, Writing – original draft, Visualization, Validation, Software, Methodology, Investigation, Formal analysis, Data curation, Conceptualization. **Alfredo Reder:** Writing – review & editing, Writing – original draft, Validation, Software, Methodology, Investigation, Formal analysis, Data curation, Conceptualization. **Guido Rianna:** Writing – review & editing, Writing – original draft, Validation, Supervision, Resources, Project administration, Methodology, Investigation, Funding acquisition, Conceptualization. **Elena Toth:** Writing – review & editing, Writing – original draft, Validation, Supervision, Resources, Project administration, Methodology, Investigation, Funding acquisition, Conceptualization.

Declaration of Generative AI and AI-assisted technologies in the writing process

The authors occasionally employed Gemini and Grammarly for targeted language editing and readability improvements during the writing process. All AI-assisted content was subsequently reviewed and verified by the authors, who remain fully responsible for the integrity and accuracy of the work.

Funding

This study was carried out within the OPERANDUM project under European Union's Horizon 2020 research and innovation programme (grant agreement No 776848), within the RETURN Extended Partnership under European Union Next-GenerationEU (National Recovery and Resilience Plan – NRRP, Mission 4, Component 2, Investment 1.3 – D.D. 1243 2/8/2022, PE0000005), and within the project "Stochastic amplification of climate change into floods and droughts change (CO22Water)" - FIS00000846 - CUP J53C23003860001. This publication is funded by the Italian Science Fund under FIS1.

Declaration of Competing Interest

The authors declare that they have no known competing financial interests or personal relationships that could have appeared to influence the work reported in this paper.

Acknowledgements

The authors acknowledge the World Climate Research Programme's Working Group on Regional Climate, and the Working Group on Coupled Modelling, former coordinating body of CORDEX and responsible panel for CMIP5. We also thank the climate modelling groups (listed in Table 1 of this paper) for producing and making available their model output. We also acknowledge the Earth System Grid Federation infrastructure, an international effort led by the U.S. Department of Energy's Program for Climate Model Diagnosis and Intercomparison, the European Network for Earth System Modelling and other partners in the Global Organisation for Earth System Science Portals (GO-ESSP).

Appendix A. Supporting information

Supplementary data associated with this article can be found in the online version at doi:10.1016/j.ejrh.2026.103864.

Data availability

Data that are not publicly available will be made available upon request.

References

Adinolfi, M., Raffa, M., Reder, A., Mercogliano, P., 2023. Investigation on potential and limitations of ERA5 Reanalysis downscaled on Italy by a convection-permitting model. Clim. Dyn. 61 (9–10), 4319–4342. https://doi.org/10.1007/s00382-023-06803-w.

Ansari, R., Grossi, G., 2022. Spatio-temporal evolution of wet–dry event features and their transition across the Upper Jhelum Basin (UJB) in South Asia. Nat. Hazards Earth Syst. Sci. 22 (2), 287–302. https://doi.org/10.5194/nhess-22-287-2022.

Barendrecht, M.H., Matanó, A., Mendoza, H., Weesie, R., Rohse, M., Koehler, J., De Ruiter, M., Garcia, M., Mazzoleni, M., Aerts, J.C.J.H., Ward, P.J., Di Baldassarre, G., Day, R., Van Loon, A.F., 2024. Exploring drought-to-flood interactions and dynamics: A global case review. WIREs Water, e1726. https://doi.org/10.1002/wat2.1726.

Berg, P., Christensen, O.B., Klehmet, K., Lenderink, G., Olsson, J., Teichmann, C., Yang, W., 2019. Summertime precipitation extremes in a EURO-CORDEX 0.11° ensemble at an hourly resolution. Nat. Hazards Earth Syst. Sci. 19 (4), 957–971. https://doi.org/10.5194/nhess-19-957-2019.

Bergström, S. (1976). Development and Application of a Conceptual Runoff Model for Scandinavian Catchments. Department of Water Resources Engineering, Lund Institute of Technology, University of Lund. https://books.google.it/books?id=vRyeQAAACAAJ.

Bertola, M., Viglione, A., Vorogushyn, S., Lun, D., Merz, B., Blöschl, G., 2021. Do small and large floods have the same drivers of change? A regional attribution analysis in Europe. Hydrol. Earth Syst. Sci. 25 (3), 1347–1364. https://doi.org/10.5194/hess-25-1347-2021.

Biella, R., Shyrokaya, A., Ionita, M., Vignola, R., Sutanto, S.J., Todorovic, A., Teutschbein, C., Cid, D., Llasat, M.C., Alencar, P., Matanó, A., Ridolfi, E., Moccia, B., Pechlivanidis, I., Van Loon, A., Wendt, D.E., Stenfors, E., Russo, F., Vidal, J.-P., Tallaksen, L.M., 2025. The 2022 drought needs to be a turning point for European drought risk management. Nat. Hazards Earth Syst. Sci. 25 (11), 4475–4501. https://doi.org/10.5194/nhess-25-4475-2025.

Blaney, H.F., & Criddle, W.D. (1962). Determining Consumptive Use and Irrigation Water Requirements. USDA Technical Bulletin 1275, US Department of Agriculture, Beltsville.

Blöschl, G., Hall, J., Parajka, J., Perdigão, R.A.P., Merz, B., Arheimer, B., Aronica, G.T., Bilibashi, A., Bonacci, O., Borga, M., Čanjevac, I., Castellarin, A., Chirico, G.B., Claps, P., Fiala, K., Frolova, N., Gorbachova, L., Gül, A., Hannaford, J., Živković, N., 2017. Changing climate shifts timing of European floods. Science 357 (6351), 588–590. https://doi.org/10.1126/science.aan2506.

Brath, A., Casagli, N., Marani, M., Mercogliano, P., & Motta, R. (2023). Rapporto della Commissione tecnico-scientifica istituita con deliberazione della Giunta Regionale n. 984/2023 e determinazione dirigenziale 14641/2023, al fine di analizzare gli eventi meteorologici estremi del mese di maggio 2023. Regione Emilia-Romagna.

Brunner, M.I., 2023. Floods and droughts: A multivariate perspective. Hydrol. Earth Syst. Sci. 27 (13), 2479–2497. https://doi.org/10.5194/hess-27-2479-2023.

Brunner, M.I., Swain, D.L., Wood, R.R., Willkofer, F., Done, J.M., Gilleland, E., Ludwig, R., 2021. An extremeness threshold determines the regional response of floods to changes in rainfall extremes. Commun. Earth Environ. 2 (1), 173. https://doi.org/10.1038/s43247-021-00248-x.

Cammalleri, C., Sarwar, A.N., Avino, A., Nikravesh, G., Bonaccorso, B., Mendicino, G., Senatore, A., Manfreda, S., 2024. Testing trends in gridded rainfall datasets at relevant hydrological scales: A comparative study with regional ground observations in Southern Italy. J. Hydrol. Reg. Stud. 55, 101950. https://doi.org/10.1016/j.ejrh.2024.101950.

Cannon, A.J., Sobie, S.R., Murdock, T.Q., 2015. Bias Correction of GCM Precipitation by Quantile Mapping: How Well Do Methods Preserve Changes in Quantiles and Extremes? J. Clim. 28 (17), 6938–6959. https://doi.org/10.1175/JCLI-D-14-00754.1.

Casanueva, A., Herrera, S., Iturbide, M., Lange, S., Jury, M., Dosio, A., Maraun, D., Gutiérrez, J.M., 2020. Testing bias adjustment methods for regional climate change applications under observational uncertainty and resolution mismatch. Atmos. Sci. Lett. 21 (7). https://doi.org/10.1002/asl.978.

Castaneda-Gonzalez, M., Poulin, A., Romero-Lopez, R., Turcotte, R., Chaumont, D., 2022. Uncertainty sources in flood projections over contrasting hydrometeorological regimes. Hydrol. Sci. J. 67 (15), 2232–2253. https://doi.org/10.1080/02626667.2022.2137415.

Chauveau, M., Chazot, S., Perrin, C., Bourgin, P.-Y., Sauquet, E., Vidal, J.-P., Rouchy, N., Martin, E., David, J., Norotte, T., Maugis, P., De Lacaze, X., 2013. Quels impacts des changements climatiques sur les eaux de surface en France à l'horizon 2070. La Houille Blanc 99 (4), 5–15. https://doi.org/10.1051/lhb/2013027.

Christensen, J.H., Larsen, M.A.D., Christensen, O.B., Drews, M., Stendel, M., 2019. Robustness of European climate projections from dynamical downscaling. Clim. Dyn. 53 (7–8), 4857–4869. https://doi.org/10.1007/s00382-019-04831-z.

Clerc-Schwarzenbach, F.M., Selleri, G., Neri, M., Toth, E., Van Meerveld, I., & Seibert, J. (2024). HESS Opinions: A few camels or a whole caravan? https://doi.org/10.5194/egusphere-2024-864.

Cornes, R.C., van der Schrier, G., van den Besselaar, E.J.M., Jones, P.D., 2018. An Ensemble Version of the E-OBS Temperature and Precipitation Data Sets. J. Geophys. Res. Atmos. 123 (17), 9391–9409. https://doi.org/10.1029/2017JD028200.

Coron, L., Thirel, G., Delaigue, O., Perrin, C., Andréassian, V., 2017. The suite of lumped GR hydrological models in an R package. Environ. Model. Softw. 94, 166–171. https://doi.org/10.1016/j.envsoft.2017.05.002.

D'Oria, M., Ferraresi, M., Tanda, M.G., 2019. Quantifying the impacts of climate change on water resources in northern Tuscany, Italy, using high-resolution regional projections. Hydrol. Process. 33 (6), 978–993. https://doi.org/10.1002/hyp.13378.

Dallan, E., Marra, F., Fosser, G., Marani, M., Formetta, G., Schär, C., Borga, M., 2023. How well does a convection-permitting regional climate model represent the reverse orographic effect of extreme hourly precipitation? Hydrol. Earth Syst. Sci. 27 (5), 1133–1149. https://doi.org/10.5194/hess-27-1133-2023.

Dankers, R., Feyen, L., 2008. Climate change impact on flood hazard in Europe: An assessment based on high-resolution climate simulations. J. Geophys. Res. Atmospheres 113 (D19), 2007JD009719. https://doi.org/10.1029/2007JD009719.

Di Paola, F., Cimini, D., De Natale, M.P., Gallucci, D., Gentile, S., Geraldi, E., Larosa, S., Nilo, S.T., Ricciardelli, E., Viggiano, M., Volini, M., Romano, F., 2026. The May 2023 flood in Emilia-Romagna and 50-year trends in extreme precipitation based on ERA5-Land. J. Hydrol. Reg. Stud. 63, 103070. https://doi.org/10.1016/j.ejrh.2025.103070.

EEA, 2020. *European climate risk assessment: Executive summary*. Publications Office. https://data.europa.eu/doi/10.2800/204249.

Evin, G., Le Lay, M., Fouchier, C., Penot, D., Colleoni, F., Mas, A., Garambois, P.-A., Laurantin, O., 2024. Evaluation of hydrological models on small mountainous catchments: Impact of the meteorological forcings. Hydrol. Earth Syst. Sci. 28 (1), 261–281. https://doi.org/10.5194/hess-28-261-2024.

Faghih, M., Brissette, F., Sabeti, P., 2021. Impact of correcting sub-daily climate model biases for hydrological studies. Hydrometeorol. Model. Approaches. https://doi.org/10.5194/hess-2021-236.

Fang, G., Yang, J., Li, Z., Chen, Y., Duan, W., Amory, C., De Maeyer, P., 2022. Shifting in the global flood timing. Sci. Rep. 12 (1), 18853. https://doi.org/10.1038/s41598-022-23748-y.

Fedele, G., Reder, A., Mercogliano, P., 2025. Statistical Downscaling over Italy using EQM: CMIP6 Climate Projections for the 1985–2100 Period. Sci. Data 12 (1), 910. https://doi.org/10.1038/s41597-025-05270-8.

Ficchì, A., Perrin, C., Andréassian, V., 2016. Impact of temporal resolution of inputs on hydrological model performance: An analysis based on 2400 flood events. J. Hydrol. 538, 454–470. https://doi.org/10.1016/j.jhydrol.2016.04.016.

Foraci, R., Tesini, M.S., Nanni, S., Antolini, G., Pavan, V., 2023. L'inquadramento meteo e idrologico degli eventi. Ecoscienza. Sostenibilità e controllo ambientale. Ecoscienza 5, 20–24. https://www.arpae.it/it/ecoscienza/numeri-ecoscienza/anno-2023/numero-5-anno-2023/alluvione-emilia-romagna.

Fosser, G., Gaetani, M., Kendon, E.J., Adinolfi, M., Ban, N., Belušić, D., Caillaud, C., Careto, J.A.M., Coppola, E., Demory, M.-E., De Vries, H., Dobler, A., Feldmann, H., Goergen, K., Lenderink, G., Pichelli, E., Schär, C., Soares, P.M.M., Somot, S., Tölle, M.H., 2024. Convection-permitting climate models offer more certain extreme rainfall projections. Npj Clim. Atmos. Sci. 7 (1), 51. https://doi.org/10.1038/s41612-024-00600-w.

Fosser, G., Khodayar, S., Berg, P., 2015. Benefit of convection permitting climate model simulations in the representation of convective precipitation. Clim. Dyn. 44 (1–2), 45–60. https://doi.org/10.1007/s00382-014-2242-1.

Fowler, K., Knoben, W., Peel, M., Peterson, T., Ryu, D., Saft, M., Seo, K., Western, A., 2020. Many Commonly Used Rainfall-Runoff Models Lack Long, Slow Dynamics: Implications for Runoff Projections. Water Resour. Res. 56 (5), e2019WR025286. https://doi.org/10.1029/2019WR025286.

Götte, J., Brunner, M.I., 2024. Hydrological Drought-To-Flood Transitions Across Different Hydroclimates in the United States. Water Resour. Res. 60 (7), e2023WR036504. https://doi.org/10.1029/2023WR036504.

Gu, X., Cheng, N., Guan, Y., Kong, D., 2025. Seasonal diversity of global flood changes and their drivers. J. Hydrol. 662, 133976. https://doi.org/10.1016/j.jhydrol.2025.133976.

Hall, J., Arheimer, B., Borga, M., Brázdil, R., Claps, P., Kiss, A., Kjeldsen, T.R., Kriaučiūnienė, J., Kundzewicz, Z.W., Lang, M., Llasat, M.C., Macdonald, N., McIntyre, N., Mediero, L., Merz, B., Merz, R., Molnar, P., Montanari, A., Neuhold, C., Blöschl, G., 2014. Understanding flood regime changes in Europe: A state-of-the-art assessment. Hydrol. Earth Syst. Sci. 18 (7), 2735–2772. https://doi.org/10.5194/hess-18-2735-2014.

He, W., Kim, S., Wasko, C., Sharma, A., 2022. A global assessment of change in flood volume with surface air temperature. Adv. Water Resour. 165, 104241. https://doi.org/10.1016/j.advwatres.2022.104241.

He, X., Sheffield, J., 2020. Lagged Compound Occurrence of Droughts and Pluvials Globally Over the Past Seven Decades. Geophys. Res. Lett. 47 (14), e2020GL087924. https://doi.org/10.1029/2020GL087924.

Hempel, S., Frieler, K., Warszawski, L., Schewe, J., Piontek, F., 2013. A trend-preserving bias correction – the ISI-MIP approach. Earth Syst. Dyn. 4 (2), 219–236. https://doi.org/10.5194/esd-4-219-2013.

Ho, M., Nathan, R., Wasko, C., Vogel, E., Sharma, A., 2022. Projecting changes in flood event runoff coefficients under climate change. J. Hydrol. 615, 128689. https://doi.org/10.1016/j.jhydrol.2022.128689.

Ionno, A., Arsenault, R., Troin, M., Martel, J.-L., Brissette, F., 2024. Impacts of climate change on flood volumes over North American catchments. J. Hydrol. 630, 130688. https://doi.org/10.1016/j.jhydrol.2024.130688.

IPCC, 2023. Contribution of working groups I, II and III to the sixth assessment report of the intergovernmental panel on climate change. In: In Core Writing Team, Lee, H., Romero, J. (Eds.), Climate change 2023: Synthesis report, pp. 35–115. https://doi.org/10.59327/IPCC/AR6-9789291691647.

Iturbide, M., Fernández, J., Gutiérrez, J.M., et al., 2022. Implementation of FAIR principles in the IPCC: the WGI AR6 Atlas repository. Sci. Data 9, 629. https://doi.org/10.1038/s41597-022-01739-y.

Kay, A., 2022. Differences in hydrological impacts using regional climate model and nested convection-permitting model data. Clim. Change 173 (1–2), 11. https://doi.org/10.1007/s10584-022-03405-z.

Kendon, E.J., Ban, N., Roberts, N.M., Fowler, H.J., Roberts, M.J., Chan, S.C., Evans, J.P., Fosser, G., Wilkinson, J.M., 2017. Do Convection-Permitting Regional Climate Models Improve Projections of Future Precipitation Change? Bull. Am. Meteorol. Soc. 98 (1), 79–93. https://doi.org/10.1175/BAMS-D-15-0004.1.

Kendon, E., Fosser, G., Murphy, J., Chan, S., Clark, R., Glen, H., Lock, A., Lowe, J., Martin, G., Pirret, J., Roberts, N., Sanderson, M., & Tucker, S. (2019). UKCP Convection-permitting model projections: Science report. Met Office.

Kendon, E.J., Prein, A.F., Senior, C.A., Stirling, A., 2021. Challenges and outlook for convection-permitting climate modelling. Philos. Trans. R. Soc. A Math. Phys. Eng. Sci. 379 (2195), 20190547. https://doi.org/10.1098/rsta.2019.0547.

Klingler, C., Schulz, K., Herrnegger, M., 2021. LamaH-CE: LArge-SaMple DAta for Hydrology and Environmental Sciences for Central Europe. Earth Syst. Sci. Data 13 (9), 4529–4565. https://doi.org/10.5194/essd-13-4529-2021.

Kreibich, H., Blauhut, V., Aerts, J.C.J.H., Bouwer, L.M., Van Lanen, H.A.J., Mejia, A., Mens, M., Van Loon, A.F., 2019. How to improve attribution of changes in drought and flood impacts. Hydrol. Sci. J. 64 (1), 1–18. https://doi.org/10.1080/02626667.2018.1558367.

Kreibich, H., De Ruiter, M.C., Goda, K., Keiler, M., Suppasri, A., Malamud, B.D., 2021. Critical research in the water-related multi-hazard field. Nat. Sustain. 5 (2), 90–91. https://doi.org/10.1038/s41893-021-00833-0.

Lang, M., Ouarda, T.B.M.J., Bobée, B., 1999. Towards operational guidelines for over-threshold modeling. J. Hydrol. 225 (3–4), 103–117. https://doi.org/10.1016/S0022-1694(99)00167-5.

Lavers, D.A., Simmons, A., Vamborg, F., Rodwell, M.J., 2022. An evaluation of ERA5 precipitation for climate monitoring. Q. J. R. Meteorol. Soc. 148 (748), 3152–3165. https://doi.org/10.1002/qj.4351.

Lema, F., Mendoza, P.A., Vásquez, N.A., Mizukami, N., Zambrano-Bigiarini, M., Vargas, X., 2025. Technical note: What does the Standardized Streamflow Index actually reflect? Insights and implications for hydrological drought analysis. Hydrol. Earth Syst. Sci. 29 (8), 1981–2002. https://doi.org/10.5194/hess-29-1981-2025.

Lemaitre-Basset, T., Collet, L., Thirel, G., Parajka, J., Evin, G., Hingray, B., 2021. Climate change impact and uncertainty analysis on hydrological extremes in a French Mediterranean catchment. Hydrol. Sci. J. 66 (5), 888–903. https://doi.org/10.1080/02626667.2021.1895437.

Li, Z., Gao, S., Chen, M., Gourley, J.J., Hong, Y., 2022. Spatiotemporal characteristics of US floods: current status and forecast under a future warmer climate. Earth's Future 10 (10), e2022EF002700. https://doi.org/10.1029/2022EF002700.

Li, J., Johnson, F., Evans, J., Sharma, A., 2017. A comparison of methods to estimate future sub-daily design rainfall. Adv. Water Resour. 110, 215–227. https://doi.org/10.1016/j.advwatres.2017.10.020.

Lindström, G., Johansson, B., Persson, M., Gardelin, M., Bergström, S., 1997. Development and test of the distributed HBV-96 hydrological model. J. Hydrol. 201 (1–4), 272–288. https://doi.org/10.1016/S0022-1694(97)00041-3.

Linvill, D.E., 1990. Calculating Chilling Hours and Chill Units from Daily Maximum and Minimum Temperature Observations. HortScience 25 (1), 14–16. https://doi.org/10.21273/HORTSCI.25.1.14.

Liu, J., Jia, J., Yang, Y., Tang, M., Xue, Y., Lu, H., 2018. Risk Assessment for Drought-flood Abrupt Alternation in the Pearl River Basin, China. In: IOP Conference Series Materials Science Engineering, 452, 022029. https://doi.org/10.1088/1757-899X/452/2/022029.

Longo-Minnolo, G., Vanella, D., Consoli, S., Pappalardo, S., Ramírez-Cuesta, J.M., 2022. Assessing the use of ERA5-Land reanalysis and spatial interpolation methods for retrieving precipitation estimates at basin scale. Atmos. Res. 271, 106131. https://doi.org/10.1016/j.atmosres.2022.106131.

Majone, B., Villa, F., Deidda, R., Bellin, A., 2016. Impact of climate change and water use policies on hydropower potential in the south-eastern Alpine region. Sci. Total. Environ. 543, 965–980. https://doi.org/10.1016/j.scitotenv.2015.05.009.

Maraun, D., 2016. Bias Correcting Climate Change Simulations—A Critical Review. Curr. Clim. Change Rep. 2 (4), 211–220. https://doi.org/10.1007/s40641-016-0050-x.

Maraun, D., Wetterhall, F., Ireson, A.M., Chandler, R.E., Kendon, E.J., Widmann, M., Brienen, S., Rust, H.W., Sauter, T., Themeßl, M., Venema, V.K.C., Chun, K.P., Goodess, C.M., Jones, R.G., Onof, C., Vrac, M., Thiele-Eich, I., 2010. Precipitation downscaling under climate change: Recent developments to bridge the gap between dynamical models and the end user. Rev. Geophys. 48 (3), RG3003. https://doi.org/10.1029/2009RG000314.

Maraun, D., & Widmann, M. (2018). Statistical Downscaling and Bias Correction for Climate Research (1a ed.). Cambridge University Press. https://doi.org/10.1017/9781107588783.

Matanó, A., Berghuijs, W.R., Mazzoleni, M., De Ruiter, M.C., Ward, P.J., Van Loon, A.F., 2024. Compound and consecutive drought-flood events at a global scale. Environ. Res. Lett. 19 (6), 064048. https://doi.org/10.1088/1748-9326/ad4b46.

Mathevet, T. (2005). Quels modèles pluie-débit globaux au pas de temps horaire? Développements empiriques et comparaison de modèles sur un large échantillon de bassins versants [Theses, Doctorat spécialité Sciences de l'eau, ENGREF Paris]. https://hal.inrae.fr/tel-02587642.

Maurer, E.P., Pierce, D.W., 2014. Bias correction can modify climate model simulated precipitation changes without adverse effect on the ensemble mean. Hydrol. Earth Syst. Sci. 18 (3), 915–925. https://doi.org/10.5194/hess-18-915-2014.

Meehl, G.A., Senior, C.A., Eyring, V., Flato, G., Lamarque, J.-F., Stouffer, R.J., Taylor, K.E., Schlund, M., 2020. Context for interpreting equilibrium climate sensitivity and transient climate response from the CMIP6 Earth system models. Sci. Adv. 6 (26), eaba1981. https://doi.org/10.1126/sciadv.aba1981.

Melsen, L.A., Addor, N., Mizukami, N., Newman, A.J., Torfs, P.J.J.F., Clark, M.P., Uijlenhoet, R., Teuling, A.J., 2018. Mapping (dis)agreement in hydrologic projections. Hydrol. Earth Syst. Sci. 22 (3), 1775–1791. https://doi.org/10.5194/hess-22-1775-2018.

Montanari, A., Nguyen, H., Rubinetti, S., Ceola, S., Galelli, S., Rubino, A., Zanchettin, D., 2023. Why the 2022 Po River drought is the worst in the past two centuries. Sci. Adv. 9 (32), eadg8304. https://doi.org/10.1126/sciadv.adg8304.

Muñoz-Sabater, J., Dutra, E., Agustí-Panareda, A., Albergel, C., Arduini, G., Balsamo, G., Boussetta, S., Choulga, M., Harrigan, S., Hersbach, H., Martens, B., Miralles, D.G., Piles, M., Rodríguez-Fernández, N.J., Zsoter, E., Buontempo, C., Thépaut, J.-N., 2021. ERA5-Land: A state-of-the-art global reanalysis dataset for land applications. Earth Syst. Sci. Data 13 (9), 4349–4383. https://doi.org/10.5194/essd-13-4349-2021.

Osuch, M., Romanowicz, R.J., Lawrence, D., Wong, W.K., 2016. Trends in projections of standardized precipitation indices in a future climate in Poland. Hydrol. Earth Syst. Sci. 20 (5), 1947–1969. https://doi.org/10.5194/hess-20-1947-2016.

Padulano, R., Reder, A., Rianna, G., 2019. An ensemble approach for the analysis of extreme rainfall under climate change in Naples (Italy). Hydrol. Process. 33 (14), 2020–2036. https://doi.org/10.1002/hyp.13449.

Parry, S., Wilby, R.L., Prudhomme, C., Wood, P.J., 2016. A systematic assessment of drought termination in the United Kingdom. Hydrol. Earth Syst. Sci. 20 (10), 4265–4281. https://doi.org/10.5194/hess-20-4265-2016.

Peredo, D., Ramos, M.-H., Andréassian, V., Oudin, L., 2022. Investigating hydrological model versatility to simulate extreme flood events. Hydrol. Sci. J. 67 (4), 628–645. https://doi.org/10.1080/02626667.2022.2030864.

Peres, D.J., Modica, R., Cancelliere, A., 2019. Assessing Future Impacts of Climate Change on Water Supply System Performance: Application to the Pozzillo Reservoir in Sicily, Italy. Water 11 (12), 2531. https://doi.org/10.3390/w11122531.

Perra, E., Piras, M., Deidda, R., Paniconi, C., Mascaro, G., Vivoni, E.R., Cau, P., Marras, P.A., Ludwig, R., Meyer, S., 2018. Multimodel assessment of climate change-induced hydrologic impacts for a Mediterranean catchment. Hydrol. Earth Syst. Sci. 22 (7), 4125–4143. https://doi.org/10.5194/hess-22-4125-2018.

Peßenteiner, S., Hohmann, C., Kirchengast, G., Schöner, W., 2021. High-resolution climate datasets in hydrological impact studies: Assessing their value in alpine and pre-alpine catchments in southeastern Austria. J. Hydrol. Reg. Stud. 38, 100962. https://doi.org/10.1016/j.ejrh.2021.100962.

Piani, C., Weedon, G.P., Best, M., Gomes, S.M., Viterbo, P., Hagemann, S., Haerter, J.O., 2010. Statistical bias correction of global simulated daily precipitation and temperature for the application of hydrological models. J. Hydrol. 395 (3–4), 199–215. https://doi.org/10.1016/j.jhydrol.2010.10.024.

Pichelli, E., Coppola, E., Sobolowski, S., Ban, N., Giorgi, F., Stocchi, P., Alias, A., Belušić, D., Berthou, S., Caillaud, C., Cardoso, R.M., Chan, S., Christensen, O.B., Dobler, A., De Vries, H., Goergen, K., Kendon, E.J., Keuler, K., Lenderink, G., Vergara-Temprado, J., 2021. The first multi-model ensemble of regional climate simulations at kilometer-scale resolution part 2: Historical and future simulations of precipitation. Clim. Dyn. 56 (11–12), 3581–3602. https://doi.org/10.1007/s00382-021-05657-4.

Poncet, N., Lucas-Picher, P., Tramblay, Y., Thirel, G., Vergara, H., Gourley, J., Alias, A., 2024. Does a convection-permitting regional climate model bring new perspectives on the projection of Mediterranean floods? Nat. Hazards Earth Syst. Sci. 24 (4), 1163–1183. https://doi.org/10.5194/nhess-24-1163-2024.

Raffa, M., Adinolfi, M., Reder, A., Marras, G.F., Mancini, M., Scipione, G., Santini, M., Mercogliano, P., 2023. Very High Resolution Projections over Italy under different CMIP5 IPCC scenarios. Sci. Data 10 (1), 238. https://doi.org/10.1038/s41597-023-02144-9.

Rashid, M.M., Wahl, T., 2022. Hydrologic risk from consecutive dry and wet extremes at the global scale. Environ. Res. Commun. 4 (7), 071001. https://doi.org/10.1088/2515-7620/ac77de.

Reder, A., Raffa, M., Padulano, R., Rianna, G., Mercogliano, P., 2022. Characterizing extreme values of precipitation at very high resolution: An experiment over twenty European cities. Weather. Clim. Extrem. 35, 100407. https://doi.org/10.1016/j.wace.2022.100407.

Requena, A.I., Nguyen, T.-H., Burn, D.H., Coulibaly, P., Nguyen, V.-T.-V., 2021. A temporal downscaling approach for sub-daily gridded extreme rainfall intensity estimation under climate change. J. Hydrol. Reg. Stud. 35, 100811. https://doi.org/10.1016/j.ejrh.2021.100811.

Reszler, C., Switanek, M.B., Truhetz, H., 2018. Convection-permitting regional climate simulations for representing floods in small- and medium-sized catchments in the Eastern Alps. Nat. Hazards Earth Syst. Sci. 18 (10), 2653–2674. https://doi.org/10.5194/nhess-18-2653-2018.

Rezvani, R., RahimiMovaghar, M., Na, W., Najafi, M.R., 2023. Accelerated lagged compound floods and droughts in northwest North America under 1.5 °C – 4 °C global warming levels. J. Hydrol. 624, 129906. https://doi.org/10.1016/j.jhydrol.2023.129906.

Rodell, M., Li, B., 2023. Changing intensity of hydroclimatic extreme events revealed by GRACE and GRACE-FO. Nat. Water 1 (3), 241–248. https://doi.org/10.1038/s44221-023-00040-5.

Samuelsson, P., Jones, C.G., Willén, U., Ullerstig, A., Gollvik, S., Hansson, U., Jansson, C., Kjellström, E., Nikulin, G., Wyser, K., 2011. The Rossby Centre Regional Climate model RCA3: Model description and performance. Tellus A Dyn. Meteorol. Oceanogr. 63 (1), 4. https://doi.org/10.1111/j.1600-0870.2010.00478.x.

Sarigil, G., Neri, M., & Toth, E. (2024, marzo 8). An Indirect Validation of National and International Gridded Precipitation Products in Northern Italy through Rainfall-Runoff Model Application. https://doi.org/10.5194/egusphere-egu24-6800.

Senatore, A., Fuoco, D., Maiolo, M., Mendicino, G., Smiatek, G., Kunstmann, H., 2022. Evaluating the uncertainty of climate model structure and bias correction on the hydrological impact of projected climate change in a Mediterranean catchment. J. Hydrol. Reg. Stud. 42, 101120. https://doi.org/10.1016/j.ejrh.2022.101120.

Shi, W., Huang, S., Liu, D., Huang, Q., Han, Z., Leng, G., Wang, H., Liang, H., Li, P., Wei, X., 2021. Drought-flood abrupt alternation dynamics and their potential driving forces in a changing environment. J. Hydrol. 597, 126179. https://doi.org/10.1016/j.jhydrol.2021.126179.

Spinoni, J., Barbosa, P., Bucchignani, E., Cassano, J., Cavazos, T., Christensen, J.H., Christensen, O.B., Coppola, E., Evans, J., Geyer, B., Giorgi, F., Hadjinicolaou, P., Jacob, D., Katzfey, J., Koenigk, T., Laprise, R., Lennard, C.J., Kurnaz, M.L., Li, D., Dosio, A., 2020. Future Global Meteorological Drought Hot Spots: A Study Based on CORDEX Data. J. Clim. 33 (9), 3635–3661. https://doi.org/10.1175/JCLI-D-19-0084.1.

Spinoni, J., Naumann, G., Vogt, J., Barbosa, P., 2015. European drought climatologies and trends based on a multi-indicator approach. Glob. Planet. Change 127, 50–57. https://doi.org/10.1016/j.gloplacha.2015.01.012.

Spuler, F.R., Wessel, J.B., Comyn-Platt, E., Varndell, J., Cagnazzo, C., 2024. ibicus: A new open-source Python package and comprehensive interface for statistical bias adjustment and evaluation in climate modelling (v1.0.1). Geosci. Model. Dev. 17 (3), 1249–1269. https://doi.org/10.5194/gmd-17-1249-2024.

Srivastava, A.K., Grotjahn, R., Ullrich, P.A., Sadegh, M., 2021. Pooling Data Improves Multimodel IDF Estimates over Median-Based IDF Estimates: Analysis over the Susquehanna and Florida. J. Hydrometeorol. 22 (4), 971–995. https://doi.org/10.1175/JHM-D-20-0180.1.

Stahl, K., Moore, R.D., Floyer, J.A., Asplin, M.G., McKendry, I.G., 2006. Comparison of approaches for spatial interpolation of daily air temperature in a large region with complex topography and highly variable station density. Agric. For. Meteorol. 139 (3–4), 224–236. https://doi.org/10.1016/j.agrformet.2006.07.004.
Strandberg, G., Bärring, L., Hansson, U., Jansson, C., Jones, C., Kjellström, E., Kolax, M., Kupiainen, M., Nikulin, G., Samuelsson, P., Ullerstig, A., & Wang, S. (2014). CORDEX scenarios for Europe from the Rossby Centre regional climate model RCA4 (Report Metereology and Climatology No. 116). SMHI.
Switanek, M.B., Troch, P.A., Castro, C.L., Leuprecht, A., Chang, H.-I., Mukherjee, R., Demaria, E.M.C., 2017. Scaled distribution mapping: A bias correction method that preserves raw climate model projected changes. Hydrol. Earth Syst. Sci. 21 (6), 2649–2666. https://doi.org/10.5194/hess-21-2649-2017.
Tarasova, L., Lun, D., Merz, R., Blöschl, G., Basso, S., Bertola, M., Miniussi, A., Rakovec, O., Samaniego, L., Thober, S., Kumar, R., 2023. Shifts in flood generation processes exacerbate regional flood anomalies in Europe. Commun. Earth Environ. 4 (1), 49. https://doi.org/10.1038/s43247-023-00714-8.
Tarek, M., Brissette, F.P., Arsenault, R., 2020. Evaluation of the ERA5 reanalysis as a potential reference dataset for hydrological modelling over North America. Hydrol. Earth Syst. Sci. 24 (5), 2527–2544. https://doi.org/10.5194/hess-24-2527-2020.
Teutschbein, C., Seibert, J., 2012. Bias correction of regional climate model simulations for hydrological climate-change impact studies: Review and evaluation of different methods. J. Hydrol. 456–457, 12–29. https://doi.org/10.1016/j.jhydrol.2012.05.052.
Themeßl, M.J., Gobiet, A., Heinrich, G., 2012. Empirical-statistical downscaling and error correction of regional climate models and its impact on the climate change signal. Clim. Change 112 (2), 449–468. https://doi.org/10.1007/s10584-011-0224-4.
Themeßl, M.J., Gobiet, A., Leuprecht, A., 2011. Empirical-statistical downscaling and error correction of daily precipitation from regional climate models. Int. J. Climatol. 31 (10), 1530–1544. https://doi.org/10.1002/joc.2168.
Tijdeman, E., Stahl, K., Tallaksen, L.M., 2020. Drought Characteristics Derived Based on the Standardized Streamflow Index: A Large Sample Comparison for Parametric and Nonparametric Methods. Water Resour. Res. 56 (10), e2019WR026315. https://doi.org/10.1029/2019WR026315.
Todaro, V., D'Oria, M., Secci, D., Zanini, A., Tanda, M.G., 2022. Climate Change over the Mediterranean Region: Local Temperature and Precipitation Variations at Five Pilot Sites. Water 14 (16), 2499. https://doi.org/10.3390/w14162499.
Tramblay, Y., Arnaud, P., Artigue, G., Lang, M., Paquet, E., Neppel, L., Sauquet, E., 2023. Changes in Mediterranean flood processes and seasonality. Hydrol. Earth Syst. Sci. 27 (15), 2973–2987. https://doi.org/10.5194/hess-27-2973-2023.
Valéry, A., Andréassian, V., Perrin, C., 2014. As simple as possible but not simpler»: What is useful in a temperature-based snow-accounting routine? Part 2—Sensitivity analysis of the Cemaneige snow accounting routine on 380 catchments. J. Hydrol. 517, 1176–1187. https://doi.org/10.1016/j.jhydrol.2014.04.058.
Vicente-Serrano, S.M., López-Moreno, J.I., Beguería, S., Lorenzo-Lacruz, J., Azorin-Molina, C., Morán-Tejeda, E., 2012. Accurate Computation of a Streamflow Drought Index. J. Hydrol. Eng. 17 (2), 318–332. https://doi.org/10.1061/(ASCE)HE.1943-5584.0000433.
Vichot-Llano, A., Raffa, M., Campanale, A., Adinolfi, M., Ceci, G., Mercogliano, P., 2026. Projected 21st Century Changes in Precipitation and Temperature Over Italy Using CMIP6 CMCC - CM2 - SR5 Model and COSMO - CLM Dynamical Downscaling. Int. J. Climatol. 46 (6), e70311. https://doi.org/10.1002/joc.70311.
Viglione, A., Parajka, J., Rogger, M., Salinas, J.L., Laaha, G., Sivapalan, M., Blöschl, G., 2013. Comparative assessment of predictions in ungauged basins—Part 3: Runoff signatures in Austria. Hydrol. Earth Syst. Sci. 17 (6), 2263–2279. https://doi.org/10.5194/hess-17-2263-2013.
Viglione, A., & Parajka, J. (2018). TUWmodel: Lumped Hydrological Model for Education Purposes. https://CRAN.R-project.org/package=TUWmodel.
Vrac, M., Friederichs, P., 2015. Multivariate—Intervariable, Spatial, and Temporal—Bias Correction*. J. Clim. 28 (1), 218–237. https://doi.org/10.1175/JCLI-D-14-00059.1.
Ward, P.J., De Ruiter, M.C., Mård, J., Schröter, K., Van Loon, A., Veldkamp, T., Von Uexkull, N., Wanders, N., AghaKouchak, A., Arnbjerg-Nielsen, K., Capewell, L., Llasat, M.C., Day, R., Dewals, B., Di Baldassarre, G., Huning, L.S., Kreibich, H., Mazzoleni, M., Savelli, E., Wens, M., 2020. The need to integrate flood and drought disaster risk reduction strategies. Water Secur. 11, 100070. https://doi.org/10.1016/j.wasec.2020.100070.
Wasko, C., Guo, D., 2022. Understanding event runoff coefficient variability across Australia using the *hydroEvents R* package. Hydrol. Process. 36 (4), e14563. https://doi.org/10.1002/hyp.14563.
Wilby, R.L., 2017. *Climate Change in Practice: Topics for Discussion with Group Exercises*. Cambridge University Press, Cambridge. https://doi.org/10.1017/9781316534588.
WMO. (2017). WMO guidelines on the calculation of climate normals. WMO Technical Report, WMO-1203, World Meteorological Organization, Geneva, Switzerland. https://library.wmo.int/doc_num.php?explnum_id=4166.
Wyser, K., van Noije, T., Yang, S., von Hardenberg, J., O'Donnell, D., Döscher, R., 2020. On the increased climate sensitivity in the EC-Earth model from CMIP5 to CMIP6. Geosci. Model. Dev. 13 (8), 3465–3474. https://doi.org/10.5194/gmd-13-3465-2020.
Yang, S., Wu, B., Zhang, R., Zhou, S., 2013. Relationship between an abrupt drought-flood transition over mid-low reaches of the Yangtze River in 2011 and the intraseasonal oscillation over mid-high latitudes of East Asia. Acta Meteorol. Sin. 27 (2), 129–143. https://doi.org/10.1007/s13351-013-0201-0.
Ye, J., Lu, Y., Yang, X., He, Z., Huang, P., Zheng, X., 2023. Bias Correction of Hourly Satellite Precipitation Products and Their Application in Hydrological Modeling in a Hilly Watershed, China. Water 16 (1), 49. https://doi.org/10.3390/w16010049.
Yevjevich, V.M., 1967. An objective approach to definitions and investigations of continental hydrologic droughts. Colorado State University.